Towards a new geological time scale: A template for improved rock-based subdivision of pre-Cryogenian time

Graham A. Shields[1*], Robin A. Strachan[2], Susannah M. Porter[3], Galen P. Halverson[4], Francis A. Macdonald[3], Kenneth A. Plumb[5], Carlos J. de Alvarenga[6], Dhiraj M. Banerjee[7], Andrey Bekker[8], Alexander Brasier[9], Partha P. Chakraborty[7], Kent Condie[10], Kaushik Das[11], Richard Ernst[12], Anthony E. Fallick[13], Hartwig Frimmel[14], Reinhardt Fuck[6], Paul F. Hoffman[15], Balz S. Kamber[16], Anton Kuznetsov[17], Ross Mitchell[18], Daniel G. Poiré[19], Simon W. Poulton[20], Robert Riding[21], Mukund Sharma[22], Craig Storey[2], Eva Stueeken[23], Rosalie Tostevin[24], Elizabeth Turner[25], Shuhai Xiao[26], Shuanhong Zhang[27], Ying Zhou[1], Maoyan Zhu[28]

[1]Department of Earth Sciences, University College London, UK; g.shields@ucl.ac.uk
[2]School of the Environment, Geography and Geosciences, University of Portsmouth, UK
[3]Department of Earth Science, University of California at Santa Barbara, USA
[4]Department of Earth and Planetary Sciences, McGill University, Canada
[5]Geoscience Australia (retired), Canberra, Australia
[6]Instituto de Geociências, Universidade de Brasilia, Brazil
[7]Department of Geology, University of Delhi, India
[8]Department of Earth and Planetary Sciences, University of California, Riverside, USA
[9]School of Geosciences, University of Aberdeen, UK
[10]New Mexico Institute of Mining and Technology, USA
[11]Department of Earth and Planetary System Sciences, Hiroshima University, Japan
[12]Department of Earth Sciences, Carleton University, Canada; Faculty of Geology and Geography, Tomsk State University, Tomsk, Russia
[13]Isotope Geosciences Unit S.U.E.R.C., East Kilbride, UK
[14]Institute of Geography and Geology, University of Würzburg, Germany
[15]Department of Earth and Planetary Sciences, Harvard University, USA; University of Victoria, Canada
[16]School of Earth and Atmospheric Sciences, Queensland University of Technology, Brisbane, Australia
[17]Institute of Precambrian Geology and Geochronology, St. Petersburg, Russia
[18]Institute of Geology and Geophysics, Beijing, China
[19]Centro de Investigaciones Geológicas–CONICET–FCNyM, (UNLP), La Plata, Argentina
[20]School of Earth and Environment, University of Leeds, UK
[21]Department of Earth and Planetary Sciences, University of Tennessee, USA
[22]Birbal Sahni Institute of Palaeobotany, Lucknow, India
[23]Department of Earth Sciences, University of St. Andrews, UK
[24]Department of Earth Sciences, University of Cape Town, South Africa
[25]Laurentian University, Sudbury, Canada
[26]Department of Geosciences, Virginia Tech, USA
[27]Institute of Geomechanics, Chinese Academy of Geological Sciences, China
[28]Nanjing Institute of Geology and Palaeontology, Nanjing, China

Abstract

Four first-order (*Hadean, Archean, Proterozoic and Phanerozoic eon*) and nine second-order (*Paleoarchean, Mesoarchean, Neoarchean, Paleoproterozoic, Mesoproterozoic, Neoproterozoic, Paleozoic, Mesozoic and Cenozoic era*) units continue to provide intuitive subdivision of geological time. Major transitions in Earth's tectonic, biological and environmental history occurred at approximately 2.5-2.3, 1.8-1.6, 1.0-0.8 and 0.7-0.5 Ga, and so future rock-based subdivision of pre-Cryogenian time, eventually by use of global stratotypes (GSSPs), will likely require only modest deviation from current chronometric boundaries (GSSAs) at 2.5, 1.6 and 1.0 Ga, respectively. Here we argue that removal of GSSAs could be expedited by establishing event-based concepts and provisional, approximate ages for eon-, era- and period-level subdivisions as soon as practicable, in line with ratification of an Ediacaran GSSP in 2004 and chronostratigraphic definition of the Cryogenian Period at c. 720 Ma in 2012. We also outline the geological basis behind current chronometric divisions, explore how they might differ in any future rock-based scheme, identify where major issues might arise during the transition, and outline where some immediate changes to the present scheme could be easily updated/formalised, as a framework for future GSSP development. In line with these aims, we note that the currently recommended four-fold Archean subdivision has not been formally ratified and agree with previous workers that it could be simplified to an informal three-fold subdivision, pending more detailed analysis. Although the ages of period boundaries would inevitably change in a more closely rock-based or chronostratigraphic scheme, we support retention of all currently ratified period names. Existing period names, borrowed from the Greek, were chosen to delimit natural phenomena of global reach. Any new global nomenclature ought to follow this lead for consistency, and so we discourage the use of supercontinent names (e.g. Rodinian, Columbian) and regional phenomena, however exceptional. In this regard, we tentatively suggest that a new period (e.g. the 'Kratian'), could precede the Tonian as the first period of the Neoproterozoic Era and we concur with previous authors that the existing Siderian Period (named for banded iron formations) would fit better as a chronostratigraphically defined period of the terminal Archean. Indeed, all pre-Cryogenian subdivisions will need more conceptual grounding in any future chronostratigraphic scheme. We conclude that improved rock-based division of the Proterozoic Eon would likely comprise a three-fold, period-level subdivision of the Paleoproterozoic Era (Oxygenian Rhyacian, Orosirian), a four-fold subdivision of the Mesoproterozoic Era (Statherian, Calymmian, Ectasian, Stenian) and potentially four-fold subdivision of the Neoproterozoic Era (pre-Tonian 'Kratian', Tonian, Cryogenian and Ediacaran). Future refinements towards an improved rock-based pre-Cryogenian geological time scale could be propoosed by new international bodies to cover the 1) pre-Ediacaran Neoproterozoic, 2) Mesoproterozoic, 3) Paleoproterozoic and 4) Archean (and Hadean) as few experts and disciplines can speak to the entire pre-Cryogenian rock record.

1. Introduction

The term 'Precambrian', or more traditionally 'pre-Cambrian' (Glaessner, 1962), is an informal geological term that refers to the time before the beginning of the Cambrian Period at c. 0.54 Ga (Peng et al., 2020). The two pre-Cambrian eonothems (Archean and Proterozoic) have long pedigrees (Sedgwick, 1845; Logan, 1857; Dana, 1872) but were introduced formally only after extensive discussion among members of the Subcommission on Precambrian Stratigraphy (SPS), which was tasked in 1966, with Kalervo Rankama as chair, with standardizing Precambrian nomenclature (Trendall, 1966). James (1978), summarising discussions within the subcommission, outlined five categories of proposal: 1) subdivision by intervals of equal duration (Goldich, 1968; see also Hofmann, 1990; 1992; Trendall, 1991); 2) subdivision by major magmatic-tectonic cycles (Stockwell, 1961; 1982); 3) subdivision by stratotypes (Dunn et al., 1966; see also Crook, 1989); 4) subdivision by breaks in the geological record defined by radiometric ages (James, 1972); and 5) subdivision based on Earth evolution concepts (Cloud, 1976). One result of those early discussions was that an approximate chronological age of 2500 Ma was assigned to the Archean-Proterozoic boundary (James, 1978). However, further subdivision of the Precambrian in a comparable manner to that achieved for younger rocks, although favoured by some (Hedberg, 1974), proved unworkable (James, 1978) due to 1) the relatively fragmentary nature of the Precambrian rock record, much of which is strongly deformed and metamorphosed, and 2) a scarcity of age-diagnostic fossils. For this reason, a mixed approach was applied: Global Standard Stratigraphic Ages (GSSAs) were introduced to subdivide Precambrian time but the absolute ages of periods were chosen to bracket major magmatic-tectonic episodes (Plumb and James, 1986; Plumb, 1991). Since that decision was ratified, all of pre-Cryogenian Earth history and its geological record has been subdivided using geochronology rather than chronostratigraphy.

The principal Precambrian subdivisions now comprise the informal Hadean and formal Archean and Proterozoic eons (Fig. 1A), which, following the GSSA concept, are defined as units of time rather than stratigraphic packages. The Hadean Eon refers to the interval with no preserved crustal fragments that followed formation of the Earth at c. 4.54 Ga (Patterson, 1956; Manhes et al., 1980). Because the Hadean Eon left no rock record on Earth (other than reworked mineral grains or meteorites), it cannot be regarded as a stratigraphic entity (eonothem) and has never been formally defined or subdivided. It is succeeded by the Archean Eon, which is usually taken to begin at 4.0 Ga and is itself succeeded at precisely 2.5 Ga by the Proterozoic Eon. The Archean Eon is informally divided into four eras (Eoarchean, Paleoarchean, Mesoarchean and Neoarchean), although a three-fold subdivision is widely favoured (van Kranendonk et al., 2012; Strachan et al., 2020). The Proterozoic Eon is currently subdivided into three eras (Paleoproterozoic, Mesoproterozoic and Neoproterozoic) and ten periods (Siderian, Rhyacian, Orosirian, Statherian, Calymmian, Ectasian, Stenian, Tonian, Cryogenian and Ediacaran). The era names were conceived after a proposal from Hans Hofmann in 1987 (Hofmann, 1992; Plumb, 1992), while the period names derive from discussions within the SPS (Plumb 1991). The three Proterozoic eras were originally proposed to begin at 2.5 Ga (Proterozoic I), 1.6 Ga (Proterozoic II) and 0.9 Ga (Proterozoic III), respectively (Plumb and James, 1986). However, the beginning of the Neoproterozoic Era was subsequently moved to 1.0 Ga in the final proposal (Plumb, 1991).

The ages of Precambrian boundaries were selected to delimit major cycles of sedimentation, orogeny and magmatism (Plumb 1991; Fig. 1A). However, knowledge has improved considerably over the past thirty years as a result of 1) increasingly precise U-Pb zircon dating, 2) improved isotopic and geochemical proxy records of tectonic, environmental and biological evolution, and 3) new rock and fossil discoveries. As a result, some of these numerical boundaries no longer bracket the events for which they were named. The International Commission on Stratigraphy (ICS) began to address the GSSA immobility problem in 2004 when they ratified the basal Ediacaran GSSP (Global Stratotype Section and Point) on the basis of the stratigraphic expression of a global chemo-oceanographic (and climatic) event in a post-glacial dolostone unit in South Australia (Knoll et al., 2004). Latest geochronology confirms that all typical 'cap dolostone' units were deposited contemporaneously at c. 635.5 Ma (Xiao and Narbonne, GTS 2020). The Ediacaran GSSP is thus one of the most highly resolved system-level divisions of the entire geological record.

The chronostratigraphic (re)definition of the Ediacaran Period (and System) replaced the provisional GSSA (650 Ma) that had been used to mark the end of the Cryogenian Period. This allowed the Marinoan 'snowball' glaciation (c. 645 – c. 635.5 Ma) to be included within the geological period that owed its name to that glaciation. The 850 Ma age marking the beginning of the Cryogenian was subsequently found to be much older than consensus estimates for the onset of widespread Sturtian 'snowball' glaciation at c. 717 Ma (Macdonald et al., 2010; Halverson et al., 2020) and so it was also removed, following a proposal from the Cryogenian Subcommission (Shields-Zhou et al., 2016). A globally correlative stratigraphic horizon at or beneath this level has not yet been proposed by the Cryogenian Subcommission, although an approximate age of c. 720 Ma for the boundary, pending a ratified GSSP, has been written into the international geological time scale. Despite the lack of a GSSP, the age revision of the Cryogenian Period by 130 million years has been quickly accepted by the geological community worldwide, presumably because it now matches the natural phenomenon for which it was named. International geological bodies have yet to tackle any other issues of non-alignment between names and ages for any other Proterozoic period despite occasional challenges, e.g. Bleeker (2004), van Kranendonk et al. (2012).

In both cases (Cryogenian and Ediacaran GSSPs), and in the case of the earlier ratification of the Precambrian-Cambrian boundary GSSP (Brasier et al., 1994), establishment of a rock-based or chronostratigraphic concept permitted relatively easy consensus around an approximate, stratigraphically calibrated age, before more prolonged and detailed discussions could take place towards eventual GSSP proposal and ratification. In the light of rapidly expanding knowledge about Precambrian Earth history, these three precedents serve to illustrate how the GSSA approach has become outdated and how it is now evident that all Precambrian subdivisions will require revision to a more natural, chronostratigraphic framework (e.g. Bleeker 2004; Van Kranendonk et al., 2012; Ernst et al., 2020). Identified shortcomings with the inflexible GSSA approach are: a) a lack of ties to the rock record and broader Earth history, b) the diachronous nature of the tectonic events on which the current scheme (Fig. 1A) is based, and c) the lack of any major sedimentological, geochemical and biological criteria that can be used to correlate subdivision boundaries in stratigraphic records. As a result, Proterozoic period nomenclature, although increasingly used in the scientific literature, is commonly out of step with the concepts or phenomena for which they were named, while the underlying basis for both era and period nomenclature is neither universally accepted nor widely understood.

An alternative stratigraphic scheme for the Precambrian was therefore revisited for discussion based on potential Global Boundary Stratotype Sections and Points (GSSPs) (Fig. 1B) (van Kranendonk et al., 2012). Following the rationale of Cloud (1972), the approach taken was to base a revised Precambrian time scale as closely as possible around geobiological events, such as changes to oceans, atmosphere, climate or the carbon cycle that would be near instantaneous compared to changes in geotectonic processes. We agree with the rationale pursued in van Kranendonk et al (2012), which followed an earlier proposal of Bleeker (2004), while noting that some newly proposed subdivisions represent a radical departure from standard practice. This is illustrated by the proposal of a new and exceptionally long 'Rodinian' Period between 1800 Ma and 720 Ma, which replaced five of the pre-existing Proterozoic periods. The principle of naming a geological period after a hypothetical supercontinent set a further precedent that is not widely accepted.

Recent progress towards, and widespread acceptance of, chronostratigraphic definitions for two Precambrian periods suggests that the international community can act expeditiously to address the infexibility of the chronometric scheme, while overcoming the confusion generated by the informal erection of new periods and unsupported concepts. This contribution outlines current understanding of Earth history in order to open up for broader consultation new recommendations around 1) a time frame for GSSA removal, 2) rock-based concepts and approximate ages for eon-, era- and possible period-level subdivision of pre-Cryogenian time, and 3) new international expert bodies to propose concepts, criteria and candidates for future GSSPs. Our aim is to explore the geological basis behind current chronometric divisions, explore how they might differ in any future rock-based scheme, identify where major issues might arise during the transition, and identify where some immediate changes to the present scheme could be easily updated/formalised, as a framework for future GSSP development. We note that this is not simply a matter of academic interest for geologists. Establishing a robust, coherent and intuitive nomenclature for Earth history is of crucial importance towards improved understanding of our planet's history for schools, universities and academia alike.

Transitioning from a purely chronometric to a chronostratigraphic scheme will inevitably place more emphasis on the rock record and on precise stratigraphic levels within key successions and their global equivalents. In this regard, we accept the arguments made by Zalasiewicz et al. (2004) that units of time and strata are, following the introduction of boundary stratotypes and points or GSSPs, interchangeable and largely superfluous. Specifically, we agree that chronostratigraphic units such as eonothem, erathem or system are confusing and argue that they are particularly inappropriate for subdividing the enormously long time intervals and relatively incomplete rock records of the pre-Cryogenian archive. As a result, we mainly use time subdivisions below (eons, eras, periods), while recalling that their precise definitions and stratigraphically calibrated ages would eventually need to be defined using a level within a global boundary stratotype section.

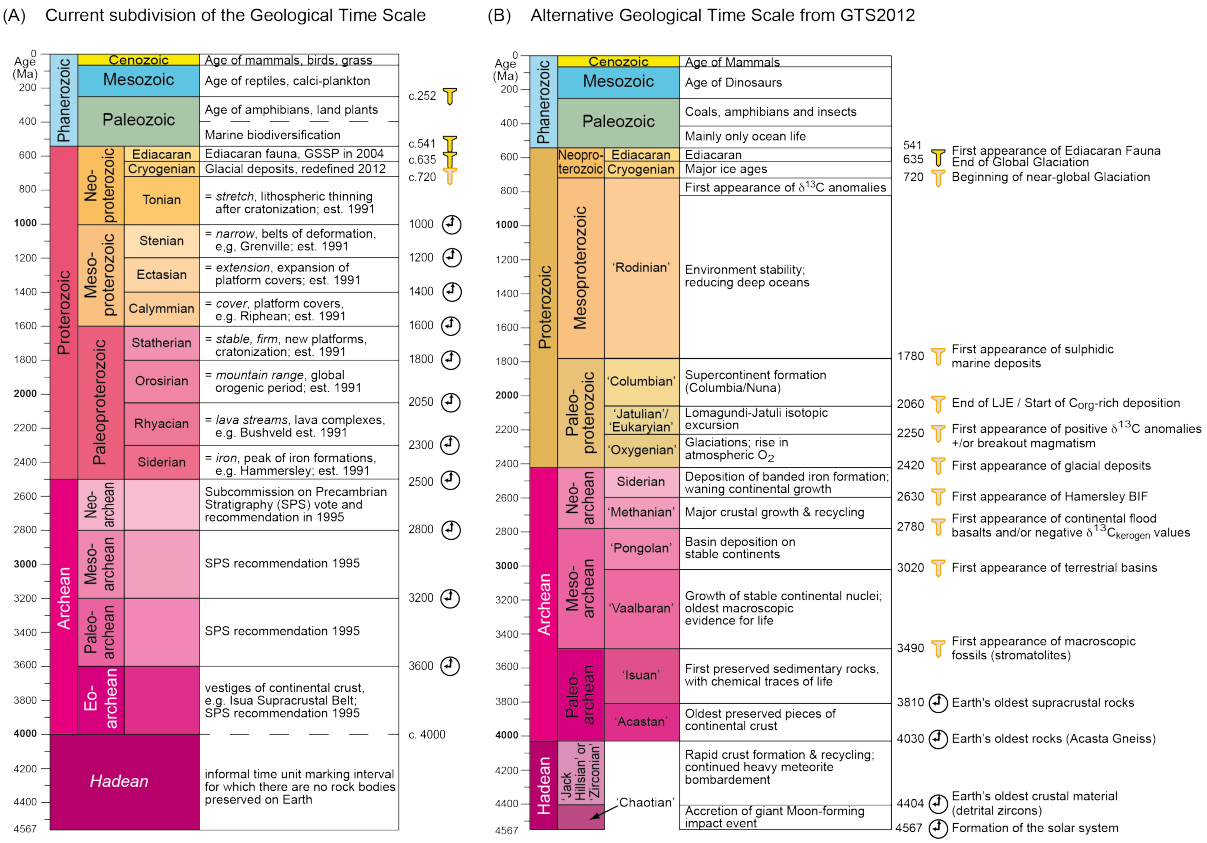

Fig. 1.*1A) Current geological time scale; 1B) Proposed Precambrian time scale using geological events (van Kranendonk et al., 2012). Golden spike symbols represent ratified (yellow) and potential (pale) GSSPs' Clock symbols represent ratified Proterozoic and recommended Archean GSSAs.*

2. Existing Eon- and Era-level subdivisions of Precambrian time

2.1 Hadean Eon (> c.4.0 Ga)

Spanning the interval between the formation of the Solar System (c. 4.567 Ga) and the first rock-based evidence for crust on Earth (c. 4.0 Ga), the Hadean Eon was a time of planetary accretion and differentiation. Defining an absolute time scale for the eon is challenging due to the criterion on which it is typically defined: the lack of a preserved rock record on Earth (Cloud, 1976; Strachan et al., 2020). Nevertheless, our understanding of the geological processes that shaped our planet during the Hadean continues to improve. Neither the beginning nor the end of the Hadean are yet formally defined by the International Commission on Stratigraphy (ICS) but the end is usually taken as 4.0 Ga (Fig. 1A). It has been proposed that the Hadean-Archaean boundary be defined as the age of the oldest preserved crustal rock (van Kranendonk et al., 2012). The oldest unambiguously dated rocks are 4.031 ± 0.003 Ga orthogneisses from the Acasta gneiss of the Slave Craton, Canada (Bowring and Williams, 1999), which led van Kranendonk et al. (2012) to propose that the boundary be placed at c. 4.03 Ga (Fig. 1B). However, other authorities have preferred a younger boundary at c. 3.85 Ga to represent the time when crustal preservation on multiple cratonic fragments increased sharply (Bleeker, 2004; Kamber, 2015).

Controversially, older ages of up to ~4.4 Ga have been inferred for mafic gneisses in the Nuvvuagittuq Supracrustal Belt in the Superior Province, Canada (O'Neil et al., 2008, 2012), based on contested interpretations of the short-lived ^{146}Sm-^{142}Nd systematics in these highly metamorphosed rocks. Zircon U-Pb ages from felsic orthogneisses in the Nuvvuagittuq Belt suggest a formation age of >3.8 Ga (e.g. Darling et al., 2014), and coupled Lu-Hf and Sm-Nd model ages of ~3.9 Ga for the mafic gneisses have been taken as evidence for an Archean, rather than Hadean origin (e.g. Guitreau et al., 2013). However, O'Neil et al. (2012) report a ^{147}Sm-^{143}Nd isochron from intrusive gabbro in the belt of 4.115 ± 0.1 Ga. Taken together, these studies highlight the difficulty in unambiguously dating highly deformed and metamorphosed ancient crustal rocks from very small preserved fragments (Kamber, 2015), while confirming that c. 4.0 Ga (or slightly later) still represents a suitable approximate age for the Hadean-Archean boundary if defined on the basis of potentially correlative rock and mineral assemblages. To debate this boundary further lies, however, beyond the scope and intent of the current paper as the defining concept of the Hadean remains unchallenged.

2.2 Archean Eon (c. 4.0 to 2.45/2.5 Ga)

The Archean Eon spans the period of early crustal formation and thickening, leading up to the formation of the first cratons and platform sedimentation. It is characterised by granite-greenstone terranes and the extrusion of ultramafic lavas (komatiites), which are very rare in post-Archean rocks. It is the "end" of granite-greenstone terranes which was traditionally used to define the upper boundary of the Archean at 2.5 Ga. Away from the recognised granite-greenstone terranes or younger platform covers, the Archean is characterised by high-grade, polymetamorphic granite-gneiss complexes, of all ages.

Subdivision of the chronometric Archean Eon was not formalised, pending collection of more data and analysis (Plumb, 1991). Nevertheless, the Subcommission on Precambrian Stratigraphy (SPS) voted subsequently in 1991 and again in 1995 to pursue formal subdivision into four eras: Eoarchean (>3.6 Ga), Paleoarchean (3.6 to 3.2 Ga), Mesoarchean (3.2 to 2.8 Ga), and Neoarchean (2.8 to 2.5 Ga) (Fig. 1A); no reasons for the choice of these boundaries were given. Since these subdivisions have not been formally ratified (Robb et al., 2004), they are considered to be recommendations only (Bleeker, 2004). An alternative subdivision scheme was proposed by van Kranendonk et al. (2012), which simplified these to three: the Paleoarchean (4.03 to 3.49 Ga), Mesoarchean (3.49 to 2.78 Ga), and Neoarchean (2.78 to 2.42 Ga), each composed of a number of periods (Fig. 1B). The base of the Paleoarchean in the 2012 proposal was defined by the age of the oldest extant rocks, the Acasta Gneiss, Canada, while the base of the overlying Mesoarchean was defined at the oldest microbially-influenced textures or structures in stromatolites of the North Pole Dome in western Australia, thus representing the oldest potential "golden spike" (Fig. 1B). The Paleoarchean contained an 'Acastan Period', the lower limit of which was defined by the oldest preserved rocks (Acasta Gneiss, Canada) and an 'Isuan Period', the lower limit of which was defined at 3.81 Ga (the age of the Earth's oldest supracrustal rocks, the Isua Supracrustal Belt in Greenland).

The problem with this approach is that the oldest occurrence of a particular rock type may identify chance preservation rather than any fundamental change in geological process, and older terrains may be identified in the future. It also runs counter to the concept of the international geological time scale as a correlative 'stratigraphic' framework. For the present, we would leave the base of the Archean at ~4.0 Ga, pending formal definition of the Hadean-Archean boundary. This argument would also seem to invalidate the Eoarchean as a fundamental unit of geological time. High grade metamorphic-plutonic complexes, with little internal stratigraphic structure (e.g., Limpopo Belt; Western Gneiss Terrains, Western Australia) become more common toward the top of the interval. A similar problem arises with the placement of the base of the Mesoarchean at c. 3.49 Ga for the North Pole Dome stromatolites; not only the problem of these being the "oldest" stromatolites, but the occurrence of stromatolites is controlled by the particular environment, rather than being a definable moment in evolution. A less ambiguous boundary for the base of the Mesoarchean could be the near-coeval base of the first preserved Barberton and Pilbara granite-greenstone terranes; clearly a significant event in Archean crustal evolution. This is currently considered to be ~3.5 Ga, or perhaps a little older.

Van Kranendonk et al. (2012) also proposed changing the end of the Archean to c. 2.42 Ga, based on the first widespread appearance of 'Huronian' glacial deposits in the rock record (Young, 2019) and the approximately contemporaneous change to an oxygenated atmosphere (Great Oxidation Event or GOE), which followed the end of the world's greatest development of banded iron formation (BIF). This approach seems reasonable based on the rock record, which supports globally significant climatic and atmospheric changes around this time (Gumsley et al., 2017). Although the GOE is sometimes taken to refer to a more prolonged interval of the early Paleoproterozoic, we restrict our usage here to this shorter interval between c. 2.45 to c. 2.32 Ga, with a preference for the earlier age (e.g. Warke et al., 2020b). The GOE has been defined in various ways but in recent years has been presumed to begin when atmospheric oxygen had accumulated sufficiently to prevent the formation and/or preservation of mass independent S-isotope fractionation in sedimentary rocks (Farquhar et al., 2000; Bekker et al., 2004). However, it is currently unclear whether this was a globally synchronous event with estimates for MIF-S disappearance varying from 2.45 to 2.32 Ga due to uncertainties over memory effects caused by oxidative weathering of sulphides and recycling of the MIF signature (Reinhard et al., 2013; Philippot et al., 2018; cf. Torres et al., 2018; Warke et al., 2020b). The MIF-S record has also shown structure within the later Archean that could potentially be used as a future stratigraphic marker (Farquhar et al., 2007; Domagal-Goldman et al., 2008; Halevy et al., 2010; Kurzweil et al., 2013) if the structure is confirmed as a global phenomenon rather than superimposed local signals (see e.g. Gallagher et al., 2017).

While the precise ages and correlation of the GOE and MIF-S events and Paleoproterozoic tillites remain uncertain (Young, 2019), an equally significant event in the transition is the end of the major late Archean BIFs. The Archean-Proterozoic boundary might be best constrained/defined by accurately dated tuffs (~2.45 Ga) at the top of the Hamersley Group BIF (Trendall et al, 2004); BIFs in the Transvaal Basin of South Africa have similar ages. This would imply redefining the Siderian Period and moving it into the Neoarchean (van Kranendonk et al., 2012); a simple solution also to the criticism that 2.5 Ga splits this important rock unit. 2.45 Ga also prevents splitting some younger classic "Archean" terranes which overlap the 2.5 Ga boundary. We note that the peak of BIF deposition would still lie in the Siderian Period should its future chronostratigraphic age match its current chronometric age (2.5 - 2.3 Ga). Therefore, we envisage two possibilities with either a terminal Archean Siderian Period ending around 2.45 Ga followed by an Oxygenian Period, or retention of the current names and approximate ages. Whichever scheme wins out will depend upon the precise criteria used to define a chronostratigraphic Archean-Proterozoic boundary, although the current authors favour the former option.

Signal reworking should not affect other geochemical or isotopic markers of upper ocean oxygenation, e.g., redox-sensitive elemental and isotopic enrichments. Geochemical signs of oxidation are recorded intermittently from the Mesoarchean (Ossa Ossa et al., 2019), becoming more expansive during the Neoarchean (Ostrander et al., 2019) and are attributed to transient pulses of oxygen prior to the GOE (the so-called 'whiffs of oxygen') (Anbar et al., 2007; Kendall et al., 2015; Stueeken et al., 2015) or more persistent oxygenation of shallow marine platform environments (Riding et al., 2014). Therefore, the Archean-Proterozoic transition interval is characterised as much by the cessation of anoxic shallow marine environments as by the onset of atmospheric oxygenation. The Neoarchean is

also remarkable for the highly negative carbon isotope composition of deposited organic carbon during the interval between c. 2.8 Ga and c. 2.6 Ga (Hayes, 1994) as well as a number of other uniquely extreme stable isotope signatures, possibly related to nascent stages of local environmental oxidation (Thomazo et al., 2009).

Complementary records of Archaean change, which can potentially be divided into three chapters, are provided by geochemical and isotopic studies of magmatic rocks that appear to indicate major secular changes in tectonic processes (Kamber and Tomlinson, 2019). On this basis, Griffin et al. (2014) concurred that the Archean Eon is best divided into: 'Paleoarchean' (4.0-3.6 Ga), 'Mesoarchean' (3.6-3.0 Ga) and 'Neoarchean' (3.0-2.4 Ga) eras. In this interpretation, during the 'Paleoarchean' Era, Earth's dominantly mafic crust acted as a stagnant-to-sluggish lid. Towards the close of the era, zircon grains reveal subtle geochemical signs of a change in tectonic regime interpreted as a move away from granitoid production from oceanic plateaus to some form of arc-like settings (Ranjan et al., 2020). It has been suggested that the subsequent 'Mesoarchean'was dominated by major episodes of mantle overturn and plume activity (van Kranendonk, 2011) that led to development of the subcontinental lithospheric mantle and a steady increase between c. 3.3 and c. 3.0 Ga in the K_2O/Na_2O ratios of TTG (tonalite-trondhjemite-granodiorite) rock suites (Johnson et al., 2019). However, early evidence of subduction is also interpreted at this time, along with diapiric doming, in adjoining terrains of the Pilbara Craton (Hickman, 2004; van Kranendonk et al., 2004).

The Neoarchean witnessed the onset of some form of plate tectonics, and the development of significant volumes of continental crust, characterised by the first K-rich granitoids (Bédard, 2018). However, gravity-driven doming and plume activity was still an active process in the formation of granite-greenstone terranes ~2720-2600 Ga (Jones et al, 2020). Progressive cratonization is reflected by the development of the first true platform covers – the Witwatersrand and Ventersdorp Supergroups from ~2.95 Ga on the Barberton Craton, the Mount Bruce Supergroup from ~2770 Ga on the Pilbara Craton and the c. 2.93 Ga to c. 2.80 Ga successions of Canada, e.g. the Steep Rock Lake Group (Riding et al., 2014). The Pongola Group (~2980 Ga) probably represents an earlier platform, but is intruded by late-tectonic granites. Emergence of this more buoyant crust may have led to these early carbonate platforms, although pre-3.0 Ga fluvial sediments imply at least some earlier regional emergence (Heubeck and Lowe, 1994). The first development of platform covers on stable cratons provides a logical interim boundary within the Archean and the base of the Neoarchean at ~3.0 Ga.

It seems significant that the youngest widespread granite-greenstone terranes (e.g., Yilgarn,, Kenoran, Bulawayan) are coeval with the basalt-rich Fortescue and Ventersdorp platform covers. This could form a basis for future 3-fold subdivision of the Neoarchean, into three periods based on the rock records of a newly defined Siderian Period (see above), the coeval Fortescue–Ventersdorp groups, and the Witwatersrand-Pongola groups, respectively, although to address period-level Archean subdivision any further lies beyond the scope of the present study.

Clear evidence for the transport of surface crustal material to the deep mantle is found in diamonds within kimberlites. Their stable isotope compositions, geochronology and mineral inclusions imply deep transport to the lower mantle of eclogitized basaltic protoliths that had interacted with seawater as long ago as 3.0 Ga (Shirey and Richardson, 2011; Schulze et al, 2013). Cratonization culminated in a globally stable "supercraton" regime around the Archean-Proterozoic boundary (Bleeker, 2003; Cawood et al., 2018). This configuration set up the lithospheric conditions, due to secular cooling of the mantle, for a switch to a full mode of plate tectonics, which arguably began with rift and drift of these Archean cratons and led eventually to amalgamation after c. 1.9 Ga of Nuna (Columbia), which is widely considered to have been a true supercontinent as opposed to a megacontinent comprising <50% of all continental area.

2.3 Proterozoic Eon (2.45/2.5 to c. 0.539 Ga)

The Archean and Proterozoic eons represent fundamentally different Earth systems and the boundary between the two is currently placed at precisely 2.5 Ga. This boundary approximates the change from an early Earth that, although still characteristically Archean (e.g. rare K-rich granitoids but widespread komatiite magmatism, granite-greenstone terranes), had gradually developed many aspects of modern tectonics, to a plate tectonic regime that was characterised by stabilized, emergent continental cratons and supercontinent cycles as well as a notable paucity of the high MgO lavas that are common throughout the Archean. The A-P boundary precedes quite closely but does not correspond precisely to

a change in surface environments from a reducing to an oxygenated atmosphere, and from wholly anoxic oceans to a more complex ocean redox structure characterised by oxic, anoxic-ferruginous and anoxic-euxinic portions. Consequently, the boundary must represent a planetary step change that significantly transformed, within 100 to 150 Myr, the Earth's biogeochemical cycles, presumably accompanied by the development of novel microbial pathways and metabolisms, leading eventually to larger and more complex (eukaryotic) forms. The Proterozoic marine sedimentary rock record is also marked by a greater diversity of authigenic minerals (Hazen, 2010; Hazen et al., 2011) and carbonate rock textures (James et al., 1998; Shields, 2002; Hodgskiss et al., 2018). The Proterozoic Eon is divided into three eras, namely the Paleo-, Meso-, and Neo-Proterozoic eras.

i. Paleoproterozoic Era (2.45/2.5 to 1.8/1.6 Ga)

The Palaeoproterozoic Era witnessed the transition from an Archean tectonic regime of scattered, small supercratons (Bleeker, 2003) to a more conventional form of plate tectonics, which resulted in formation of Earth's earliest widely accepted supercontinent, Nuna (Hoffman, 1989; Rogers and Santosh, 2002; Zhao et al., 2002; Evans and Mitchell, 2011; Zhang et al., 2012)), as evidenced by ~2.0-1.8 Ga orogenic belts on all of present-day continents. Redefining the Siderian to contain within in it the BIFs at the top of the Neoarchean requires a new period to be defined and named for the earliest Paleoproterozoic; van Kranendonk et al. (2012) refer to this period as the Oxygenian Period.

The Paleoproterozoic sedimentary record provides clues to significant events, some of which are likely to have been global in scale and can probably be related to the large-scale tectonic processes outlined above. Abundances of molybdenum, uranium, selenium, sulfate and iodate increased in marine sedimentary rocks in multiple Paleoproterozoic basins, indicating increasing ocean reservoirs of those redox-sensitive species (Scott et al., 2008; Partin et al., 2013; Kipp et al., 2017; Hardisty et al., 2017; Blättler et al., 2018). This trend has been interpreted as evidence of oxidative weathering caused by atmospheric oxygenation after the GOE together with expansion of oxic conditions in the marine realm, which stabilised these elements as oxyanions in solution, while titrating redox-sensitive iron, manganese and cerium out of solution (Tsikos et al., 2010; Warke et al., 2020a). Accumulation of iron formations (IFs) peaked around the Archean-Proterozoic boundary, but continued until c. 1.8 Ga (Klein, 2005), after which major BIF deposits are scarce but not entirely absent (Bekker et al., 2010; 2014; Canfield et al., 2018). The decline in the abundance of BIF is widely attributed to the titration of ferrous iron from the oceans as pyrite, following the onset of oxidative sulphide mineral weathering after the GOE (Canfield, 1998; Poulton and Canfield, 2011), although hydrothermal sources of iron may have diminished after c. 1.8 Ga (Cawood and Hawkesworth, 2014). The disappearance of redox-sensitive detrital minerals, such as pyrite, uraninite and siderite, has long been attributed to the GOE (Holland, 1984, 2006; Frimmel, 2005; van Kranendonk et al., 2012), although the onset and duration of the GOE is still inadequately constrained (e.g. Luo et al., 2016) and may not have been synchronous everywhere (Phillipot et al., 2018; Hodgskiss et al., 2019). The onset of the GOE is generally considered to have been approximately contemporaneous with what some have interpreted as the Earth's first global scale glaciations (Bekker and Kaufman, 2007; Brasier et al., 2013; Tang and Chen, 2013; Bekker, 2014; Young, 2019). However, the strongest evidence for a Paleoproterozoic Snowball Earth comes from South Africa where evidence of low-latitude glaciation in the Makganyene Formation (Evans et al., 1997) is found below the first evidence of atmospheric oxygenation (Guo et al., 2009).

Paleoproterozoic glacial episodes were followed by the Earth's largest known positive $\delta^{13}C$ excursion (or excursions, see Martin et al., 2015), the Lomagundi-Jatuli Event (LJE) between c. 2.31-2.22 and c. 2.11-2.06 Ga (Martin et al., 2013), which accompanied the first major evaporite sulfate deposits (Melezhik et al., 2005; Schröder et al., 2008; Brasier et al., 2011; Blättler et al., 2018). The LJE is followed by the c. 2.06 Ga Shunga Event that is characterised by a major accumulation of C_{org}-rich sedimentary rocks, the generation of giant petroleum deposits (Melezhik et al. 2004) and pyrite-rich black shale (Sheen et al., 2019) as well as the first sedimentary phosphorite deposits (Kipp et al., 2020). The c. 2.06 Ga Shunga Event interestingly coincides with the emplacement of two Large Igneous Provinces (LIPs), the Bushveld LIP (Kaapvaal craton) and the Kevitsa LIP on the Karelian craton (e.g. Ernst et al. 2020), which inspired the name of the chronometric Rhyacian Period (2.3 – 2.05 Ga) after the Greek word Rhyax (meaning streams of lava) (Plumb, 1991). One potentially distinctive feature of the middle Paleoproterozoic is a disputed tectono-magmatic lull between c. 2.3 to 2.2 Ga (Spencer et

al., 2018), during which evidence of continental magmatism and orogenesis is scarce, but not entirely absent (Partin et al., 2014; Moreira et al., 2018). Juvenile magmatism reinitiated after c. 2.2 Ga (Condie et al., 2009; Spencer et al., 2018).

The first macroscopic organic-walled fossils, coiled forms similar to *Grypania spiralis*, appear within Paleoproterozoic strata by c. 1.89 Ga (Han and Runnegar, 1992; Javaux and Lepot, 2018) to be joined by large, more convincingly eukaryote-grade fossils by the end of the era (Zhu et al., 2016). The Paleoproterozoic fossil record contains the c. 1.88 Ga Gunflint fossil microbes, which are taken to be the oldest unambiguous evidence of iron-oxidising bacteria and oxygenic cyanobacteria (Planavsky et al., 2009; Crosby et al., 2014; Lepot et al., 2017), although cyanobacterial fossils are known also from the c. 2.0 Ga Belcher Group in eastern Hudson Bay (Hofmann, 1975; Hodgskiss et al., 2019).

A period of worldwide orogeny and major crustal growth from c. 2.06 to 1.78 Ga, and reaching maximum intensity between 1.90-1.85 Ga, (Condie, 1998, 2004; Puetz and Condie, 2019; Condie and Puetz, 2019) culminated in the formation of the supercontinent Nuna or Columbia (Zhao et al., 2002), speculated to have been Earth's first "true" supercontinent (Hoffman, 1989; Bleeker, 2003; Mitchell, 2014). For example, Nuna assembly is largely constrained to between ca. 2.0-1.8 Ga, from the 1970 Ma Thelon orogen (Bowring and Grotzinger, 1992), with the Rae craton serving as the upper plate of the growing Laurentia (Hoffman, 2014) that was central to Nuna (Evans and Mitchell, 2011). Local orogeny continued through the Statherian, culminating with final suturing events in northern Australia during the early Calymmian (ca. 1.6-1.5 Ga) (Pourteau et al., 2018; Gibson et al., 2020), which was peripheral in Nuna (Kirscher et al., 2019).

The end of the Paleoproterozoic Era, as currently defined, is characterised by the widespread formation of unmetamorphosed, shallow-marine sedimentary basins with expansive carbonate platforms over increasingly stable cratons, following amalgamation of Nuna. Some such as the c.1.7–c. 1.4 Ga Changcheng-Jixian groups of the Sino-Korean or North China craton, are traditionally considered and mapped as Mesoproterozoic successions (Zhao and Cawood, 2012), despite their slightly earlier origin prior to 1.6 Ga. Many other classic mid-Proterozoic sequences also fall into this category, having begun their depositional history similarly during the chronometric Statherian Period (1.8-1.6 Ga). For example, pre-1.6 Ga units originally envisaged to fall within the chronometric Proterozoic II (Plumb and James, 1986: Figure 1) include the McArthur Basin of Australia (Rawlings, 1999); the lower Riphean Burzyan Group of Russia (Semikhatov et al., 2015); the Espinhaço Supergroup and Araí Group of Brazil and coeval Chela Group of central Africa (Chemale et al., 2012; Guadagnin et al., 2015; Pedreira and de Waele, 2008); the Vindhyan and Cuddupah supergroups of India (Ray, 2006; Chakraborty et al., 2020); and the Uncompahgre Group of SW Colorado, USA, which formed during the late stages of the Yavapai orogeny (1.71-1.68 Ga) (Whitmeyer and Karlstrom, 2007).

The difficulty in assigning a precise age for the Paleoproterozoic - Mesoproterozoic boundary due to the prolonged nature of late Paleoproterozoic orogenies, now known to relate to the amalgamation of Nuna, was recognized early on by the Precambrian Subcommission who expressed "*individual preferences ... from 1400 Ma to 1800 Ma*" (Plumb and James, 1986). In this contribution, we recommend that the end of the Paleoproterozoic be provisionally redefined as ~1.8 Ga, and the Statherian be placed in the Mesoproterozoic, pending future definition of GSSPs. This age is constrained by the latest Orosirian magmatic activity dated at ~1.82 Ga and the base of first platform covers ~1.8 Ga.

ii. Mesoproterozoic Era (1.8/1.6 to c. 1.0 Ga)

The Mesoproterozoic Era represents a period of seeming overall stability in Earth history, during which there were long thought to be few changes in the sedimentary record, biogeochemical cycling, climate and biological evolution (Buick et al., 1995; Brasier and Lindsay, 1998). New platform covers, soon after Orosirian orogeny, developed across most cratons. For example, the McArthur Basin of North Australia saw up to 10 km of sediments deposited throughout the period from 1.8-1.6 Ga: the Tawallah Group of sandstone and volcanics volcanics from ~1.8-1.7 Ga, succeeded by stromatolitic and evaporitic carbonates of the McArthur Group, ~1.7-1.6 Ga. The near basal mafic volcanics and intrusives across the coeval Tawallah and Kimberley Groups represent the major extensional Carson LIP. Detailed studies show significant breaks throughout which correlate with changes in direction in a polar wander curve from the same sections, illustrating active plate tectonic control of basins near craton

margins (Idnurm et al., 1995, Page et al, 2000). Relatively thin sandstone-volcanic sequences were initiated about the same time in Brazil and central Africa, but did not continue up into carbonates (Pedreira et al., 2008). The arenitic Changcheng Group of China began later, after ~ 1.7 Ga, and continued through the carbonate-rich Jixian Group until after ~1.44 Ga (Qu et al., 2014), as did the Lower Riphean of Russia (Semikkatov et al, 2015).

The final assembly of Nuna was completed at ~1.5 Ga (Pourteau et al., 2018; Gibson et al., 2020) and followed soon after by thick terrigenous deposition in the Roper (North Australia) and Belt-Purcell (western North America) Basins. The period 1.4–1.25 Ga saw few, short-lived basins worldwide, and was dominated by the breakup of the core of supercontinent Nuna (Evans and Mitchell, 2011) although the breakup may have been relatively incomplete (Ernst et al., 2016; Li et al., 2019) as it was likely followed by re-amalgamation into a different configuration by around 1.0 Ga to form the supercontinent Rodinia (Li et al., 2008). This partial breakup could be reflected in the 1.33-1.30 Ga Derim Derim-Yanliao LIP of northern Australia and the North China craton (Bodorkos et al, 2020).

The final period of the Mesoproterozoic was named Stenian for the "Grenvillian" worldwide linear orogenic belts (Plumb, 1991). The type Grenvillian is specifically defined by two events: Boundary, ~1090 – 1020 Ma and Rigolet, ~1000 – 980 Ma (Rivers, 2015). The Boundary event was probably the time of collision and is defined by high-grade metamorphic rocks from deep in the crust. The Rigolet boundary was a higher-level event with less movement. An extensional event separated the two, and magmatic emplacement of anothosites, charnockites and metagranites occurred throughout. Earlier events, integral to the belt, extend back to c. 1200 Ma. The Sunsás and Natal-Namaqua belts display similar deep-seated metamorphism and magmatism between c. 1200 – 1000 Ma (Cornell et al., 2006; Teixeira et al., 2010). However, in Central Australia, the high-grade 1240-1120 Ma Musgrave Orogeny is followed by the Warkuma LIP. The mafic-ultramafic Giles Complex was emplaced at various levels into the metamorphic rocks, coeval with high-evel p[ost-tectonic granites and the bimodal Bentley Supergroup (Howard et al, 2014).

Increasingly convincing discoveries of fossil eukaryotes, in the form of large, multicellular organic-walled fossil fronds and ornamented acritarchs (Zhu et al., 2016; Miao et al. 2019), first occur in rocks that straddle the chronometric Paleoproterozoic–Mesoproterozoic boundary at 1.6 Ga, and suggest that much of the Mesoproterozoic fossil record remains undiscovered. Current fossil and molecular evidence agree that crown group Archaeplastida (a group that includes the red, green and glaucophyte algae) emerged during the Mesoproterozoic Era (Butterfield, 2000; Eme et al. 2014), or possibly even earlier in non-marine environments (Sánchez-Baracaldo et al., 2017). Multicellular eukaryotic algae appear before 1.0 Ga in the form of isolated examples of red algae (*Bangiomorpha pubescens* at c. 1.05 Ga) and green algae (*Proterocladus antiquus* at c. 1.0 Ga) (Butterfield et al., 1994; Tang et al., 2020), although see possibly earlier examples of red algae from India (*Rafatazmia chitrakootensis* and *Ramathallus lobatus)* at c. 1.6 Ga (Bengtson et al., 2017). Ornamented acritarchs are more common eukaryote-grade fossils and some may prove useful for biostratigraphy, e.g. *Tappania plana* is a widely reported Mesoproterozoic fossil taxon, which has been found in the Ruyang Group of China (Yin, 1997; Yin et al., 2018), Roper Group of Australia (Javaux et al., 2001; Javaux and Knoll, 2017); Siberia (Nagovitsin, 2009), USA (Adam et al., 2017) and Singhora Group, India (Singh et al., 2019). Therefore, the Mesoproterozoic Era, although often given the epithet 'boring', marks the point in geological time when biostratigraphy begins to seem possible.

As summarised by Cawood and Hawkesworth (2014), the period from 1.7 to 0.75 Ga is characterised by a paucity of passive margins (Bradley, 2008), anoxic-ferruginous and regionally euxinic marine environments, an absence of significant Sr isotope deviations in the seawater record, few highly evolved $\varepsilon_{Hf(t)}$ values in zircon grains, limited orogenic gold and VHMS (but major sedimentary exhalative Pb-Zn) deposits, an absence of glacial deposits and a paucity of massive BIF. Although thought to be Paleoproterozoic in age (Bekker et al., 2003; Papineau, 2010), some of the oldest significant phosphorite deposits may instead have formed around the 1.6 Ga mark in India and Australia (McKenzie et al., 2013; Crosby et al., 2014; Chakraborty et al., 2020; Fareeduddin and Banerjee, 2020). Anorthosites and related intrusive rocks are characteristic of the middle Mesoproterozoic (c. 1.5 – 1.2 Ga) and are in places spatially and temporally linked to convergent plate margins (Whitmeyer and Karlstrom, 2007; McLelland et al., 2010; Ashwal and Bybee, 2017). Their development during the Mesoproterozoic was attributed by Cawood and Hawkesworth (2014) to

secular cooling of the mantle to a temperature at which continental lithosphere was strong enough to be thickened, but still warm enough to result in melting of the lower thickened crust.

A lack of stratigraphically useful new life forms, major climatic changes, and demonstrably global C isotope excursions throughout the Mesoproterozoic makes it particularly difficult to subdivide. However, the Mesoproterozoic C-isotope record may have been less invariant than has been appreciated until now as exceptions to the apparent montony are emerging (e.g. Zhang, K. et al., 2018; Shang et al., 2019). Regional scale magmatic events such as the c. 1320 Ma and c. 1230 Ma dyke swarms of North China (Zhai et al., 2015; Peng et al., 2015; Wang et al., 2016), the Mackenzie dyke swarm in Canada (c. 1.27 Ga) and the approximately contemporaneous Ghanzi-Chobe-Umkondo and Midcontinent Rift Systems (c. 1.12-1.08 Ga) have not been linked to any global-scale isotopic excursions that could be used for correlation, although the coincidence of widespread ca. 1385 Ma LIPs and black shales has been proposed as potential rock-based markers of Mesoproterozoic subdivision, e.g., at the Calymmian-Ectasian boundary (Zhang, S. et al., 2018).

The final period of the Mesoproterozoic was named 'Stenian' for a series of orogenies (Plumb, 1991) that led eventually to formation of the supercontinent Rodinia, which completed its final amalgamation phase by c. 950 Ma (Li et al., 1999; Evans et al., 2016). The first period of the Neoproterozoic was named 'Tonian', due to the lithospheric stretching now known to be related to the break-up of Rodinia, and originally placed at 0.9 Ga (Plumb and James, 1986).

iii. Neoproterozoic Era (c.1.0 – c.0.54 Ga)

The subdivision of Neoproterozoic time has largely been informed by 1) the occurrence of widespread glacial units now known to be of late Precambrian age (Thomson, 1871; 1877; Reusch, 1891; Kulling, 1934; Lee, 1936; Mawson, 1949) and 2) fossils of metazoan affinity that postdate those glaciogenic deposits but predate Cambrian strata (Glaessner, 1962). Harland (1964) first proposed the term "infra-Cambrian" or "Varangian" for the late Precambrian system (Fig. 2) based on two discrete diamictite units, the Smalfjord (Bigganjargga) and Mortensnes, although these are now known to be of late Cryogenian (Marinoan) and Ediacaran age, respectively. Harland proposed that the start of this new period should correspond to the base of the lower of these two glacial horizons on the Varanger Peninsula, NE Norway, first described by Reusch (1891). Dunn et al. (1971) subsequently introduced the terms "Sturtian" and "Marinoan" (named after Sturt Gorge and Marino Rocks near Adelaide) for the two glacial epochs recorded in the late Proterozoic strata of the Adelaide Geosyncline of South Australia, emphasizing their utility as chronostratigraphic markers. Cloud and Glaessner (1982) proposed the term "Ediacarian" for the interval spanning from the upper limit of the last late Precambrian glacial deposit to the base of the Cambrian. This term also originates from South Australia (the Ediacaran Hills) where Ediacara-type fossils were recognized (Sprigg, 1947). Plumb (1991) penned the name "Cryogenian" for the period that included the more widespread of the late Neoproterozoic ice ages and the term "Tonian" (meaning stretching in Greek and in reference to the onset of rifting, now related to the break-up of Rodinia) for the preceding period, setting the chronological boundary between them at precisely 850 Ma. These terms and GSSA boundaries were revised from previously suggested period-rank subdivisions on the geological time scale by the Subcommission on Precambrian Stratigraphy (Plumb and James, 1986).

The number, duration, and intensity of the glaciations have been intensely debated (e.g., Kaufman et al., 1997; Kennedy et al., 1998; Halverson et al., 2005), particularly in the light of the Snowball Earth hypothesis (Hoffman et al., 1998; Hoffman and Schrag, 2002; Fairchild and Kennedy, 2007; Etienne et al., 2007). Notwithstanding these debates, the base of the Ediacaran System (Period) was formally ratified in 2004 in the Adelaide Geosyncline (Knoll et al., 2004; 2006) at the same stratigraphic level as originally proposed by Cloud and Glaessner (1982) for their "Ediacarian" period. The terms Cryogenian and Tonian are now widely accepted for the two preceding periods (Shields-Zhou et al., 2012, 2016). Recent proliferation of radioisotopic ages spanning Neoproterozoic glacial deposits has largely resolved the question of the number and timing of late Precambrian glacial intervals. It is now well established that two discrete glaciations of global extent occurred during the Cryogenian Period (i.e., between c. 717 Ma and c. 635 Ma). Despite initial reservations, the international community generally uses the terms *Sturtian* and *Marinoan* to refer to these two glacial events ("cryochrons", cf. Hoffman et al., 2017) of the Cryogenian Period. This subdivision, though still

informal, appears justifiable in light of the geochronological evidence that 1) the Sturtian glaciation is now thought to have begun at c. 717 Ma (Macdonald et al., 2010, 2018; McLennan et al., 2018) and ended at c. 660 Ma (Rooney et al., 2015; 2020; Cox et al., 2018; Wang et al., 2019) synchronously worldwide, within the uncertainty of available ages, and that 2) the Marinoan glaciation, though shorter-lived and of uncertain duration (between about 4 and 17 Myr; Hoffmann et al., 2004; Condon et al., 2005; Prave et al., 2016; Nelson et al., 2020) also ended synchronously at c. 635.5 Ma (Crockford et al., 2018; Zhou et al., 2019). The start of the Cryogenian Period has now been changed to c. 720 Ma so as to encompass only the glacigenic sequences, pending proposal and ratification of a GSSP.

The preceding Tonian Period now lasts 280 million years. Having originally been envisaged to encapsulate a period of lithospheric thinning (supercontinent break-up), the Tonian now covers the final amalgamation of Rodinia (Evans et al., 2016) and a prolonged interval of relative stability prior to the onset of major break-up after 0.85 Ga, and perhaps as late as 0.75 Ga (Jing et al., 2020).

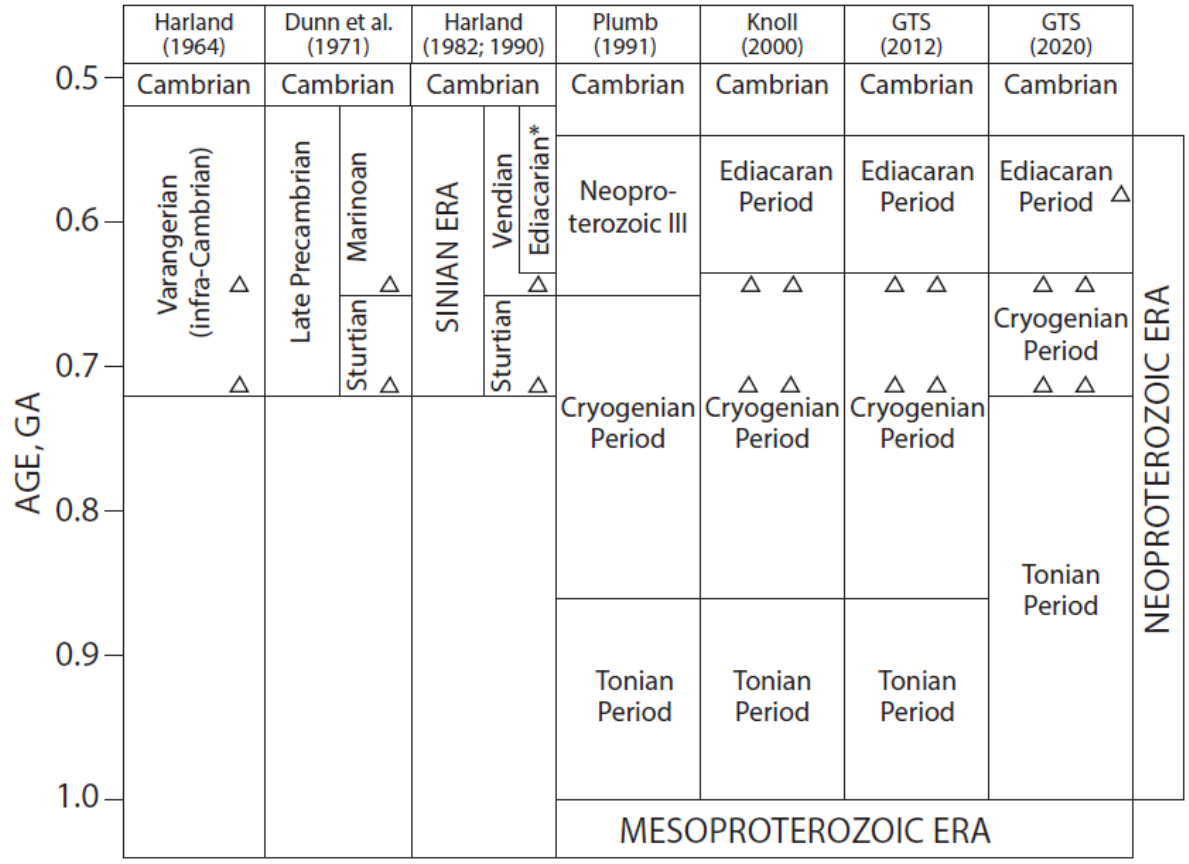

Fig. 2. *Evolution of stratigraphic terminology for the Neoproterozoic Era. Note that age ranges for earlier subdivisions are based on current age estimates. Triangle symbol (Δ) denotes the approximate levels of glaciations relevant to the time scale subdivisions. * Denotes the term "Ediacarian" introduced by Cloud and Glaessner (1982).*

A proliferation of sedimentary basins in Rodinia between c. 850 and c. 800 Ma (e.g. the Centralian Superbasin of Australia; the East-Svalbard-East Greenland basin, and the Mackenzie Mountains-Amundsen and associated basins of northern-northwestern Canada, the Nanhua rift basin of South China, and the Central Africa Copperbelt (Lindsay, 2002, Hoffman et al., 2012; Rainbird et al., 1996; Wang et al., 2011; Bull et al., 2011; Li et al., 2013) was originally interpreted to record an initial phase of Rodinia break-up (Li et al., 1999; Macdonald et al., 2012), perhaps related to insulation of the underlying mantle (Lindsay, 2002) and/or the influence of a series of similarly aged mantle plumes and associated LIP events that impinged on Rodinia at this time (Li et al., 1999, 2003). The existence of widespread basin-scale evaporite deposits with ages ranging from c. 830 to c. 730 Ma (Prince et al.,

2019) is consistent with rifting around this time. However, aside from the western margin of North America (e.g. Macdonald et al., 2012; Timmons et al., 2001; Jefferson et al., 1998) evidence of extension leading to continental separation is lacking and true break-up probably began in earnest only around the start of the Cryogenian (e.g. Merdith et al., 2017), followed by a peak in passive margin abundance at c. 600 Ma (Bradley, 2008). Therefore, Rodinia's tenure as a supercontinent coincided with the Tonian Period, as currently defined, which was named for the tectonic stretching that led to its break-up. Division of the long Tonian into two periods is therefore desirable, although at present many of these c. 850-800 Ma basins lack adequate geochronological control.

3. Tracers of crustal evolution: cornerstone of the geological time scale

Recent research has focused on understanding episodicity and secular trends in the Precambrian geological record, recognising that the supercontinent cycle and mantle dynamics exert a fundamental control on the evolution of not only the Earth's lithosphere, but also the atmosphere and biosphere, including the spatial distribution of elements and therefore the evolution of mineral deposits (e.g. Huston et al., 2016; Frimmel, 2018), via a series of complex, and incompletely understood, feedbacks (e.g. Worsley et al., 1985; Lindsay and Brasier, 2002; Cawood et al., 2013; Young 2013; Grenholm and Schersten, 2015; O'Neill et al., 2015; Hawkesworth et al. 2016; van Kranendonk and Kirkland 2016; Gumsley et al., 2017; Nance and Murphy 2018; Alcott et al., 2019).

Various workers have proposed that the Precambrian can be divided into a number of major intervals based on the dominant tectonic process at any one time. Hawkesworth et al. (2016) suggested five intervals: 1) initial accretion, core/mantle differentiation, development of magma ocean and an undifferentiated mafic crust; 2) plume-dominated tectonics (pre-subduction) at c. 4.5–3.0 Ga; 3) stabilisation of cratons and onset of "hot subduction" between c. 3.0 and c. 1.7 Ga; 4) the "boring billion" at 1.7–0.75 Ga; and 5) Rodinia breakup and development of "cold subduction" from 0.75 Ga onwards. Similarly, van Kranendonk and Kirkland (2016) suggested five intervals, each of which starts with a pulse of mafic-ultramafic magmatism, includes the formation of a supercontinent, and ends with an often protracted period of relative quiescence as the previously formed supercontinent drifts and breaks apart. Following c. 4.03–3.20 Ga – the period from the start of the preserved rock record to the onset of modern-style plate tectonics – these stages are: 1) 3.20–2.82 Ga – the onset of modern-style plate tectonics and the oldest recognised Wilson cycle; 2) 2.82–2.25 Ga – commencing with major crustal growth, emergence of the continents and formation of Superior-type BIFs, and closing with magmatic slowdown and stagnant-lid behaviour; 3) 2.25–1.60 Ga – global mafic/ultramafic magmatism followed by global terrane accretion and the formation of Nuna; 4) 1.60–0.75 Ga – the "Boring Billion" but included partial break-up of Nuna and subsequent formation of Rodinia during the Grenville and other orogenies; 5) 0.75 Ga to present – breakup of Rodinia, the Pangean supercontinent cycle and present transition to Amasia (Safonova and Maruyama 2014; Mitchell et al., 2012).

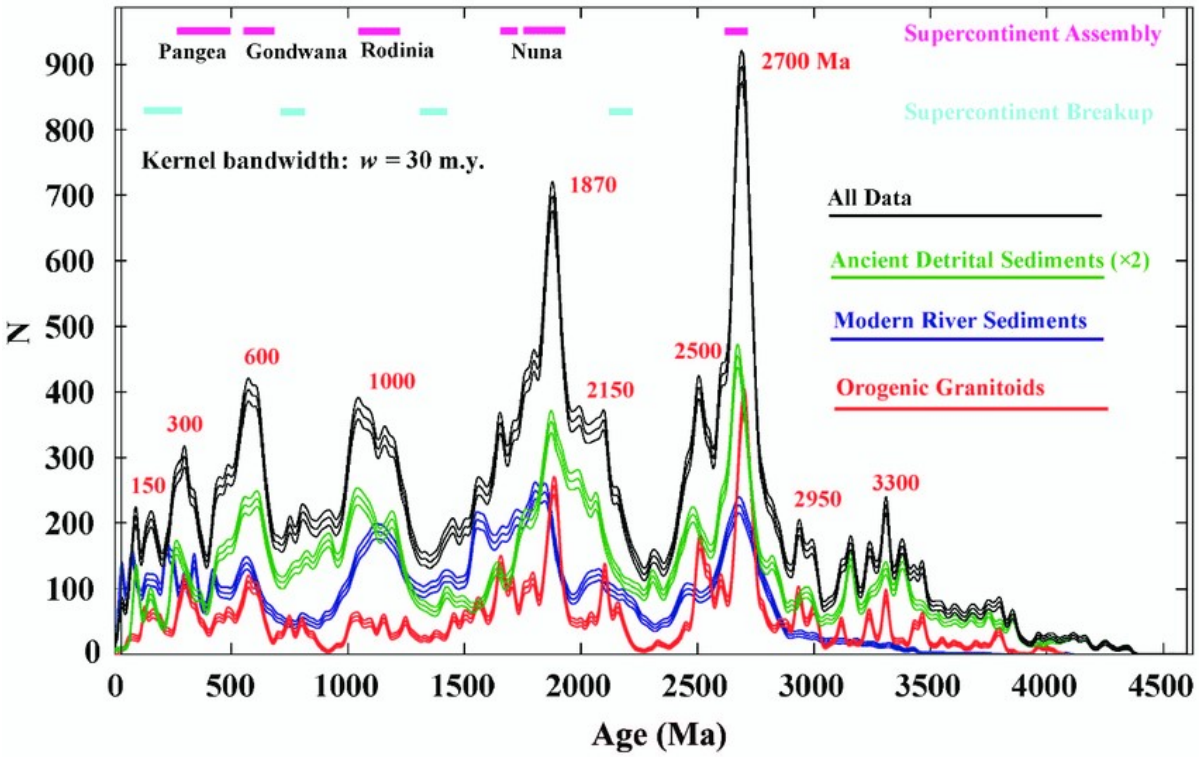

Fig. 3. *Peaks in the distribution (1σ error) of U–Pb zircon ages for orogenic granitoids and detrital zircon grains match intervals of supercontinent assembly, whereas troughs correspond to intervals of supercontinent tenure and break-up (from Condie and Aster 2010; Condie, 2014). Black: Total ages (n = 37,830); Green: detrital ancient sedimentary rocks (n = 21,849); Blue: detrital modern sediments (n = 7053; 2x); Red: orogenic granitoids (n = 8928). N (vertical axis) is the number of zircon ages as a function of time for a Gaussian kernel bandwidth of three standard deviations (30 m.y.).*

Worsley et al. (1985) and Nance et al. (1986) pointed out that processes associated with the supercontinent cycle can be tracked by several isotopic proxies. For example, the distribution of U-Pb zircon ages for the past 4.0 Ga (Fig. 3) in orogenic granitoids and detrital sedimentary rocks record similar peaks at 2.7 Ga (and 2.5 Ga), 1.87 Ga, 1.0 Ga, 0.6 Ga and 0.3 Ga, which correspond to the times of global-scale collisional orogenesis and magmatism associated with the amalgamations of Kenora (Kenorland), Nuna (Columbia), Rodinia, Pannotia/Gondwana and Pangea, respectively. A more recent compilation (Condie and Puetz, 2019) interprets these peaks to be pulses of crustal growth and revises the timing of later peaks to 1875 Ma, 1045 Ma, 625 Ma, 265 Ma and 90 Ma. A kernel density estimation analysis (Vermeesch et al., 2016) of almost 600,000 detrital zircons (Spencer et al., 2020) confirms similar peaks at 2.69 Ga, 2.50 Ga, 1.86 Ga, 1.02 Ga, 0.61 Ga, 0.25 Ga and 0.1 Ga, and troughs at 2.27 Ga, 1.55-1.28 Ga, 0.88-0.73 Ga, 0.38 Ga and 0.20 Ga. Variations in the mean initial εHf and $\delta^{18}O$ values from detrital zircon grains in recent sediments show negative troughs and positive peaks, respectively, that correspond to times of supercontinent assembly (Fig. 3). Both proxies are consistent with extensive crustal re-working at the time of assembly with more juvenile contributions representing times of supercontinent breakup and dispersal. Most importantly, all current major subdivisions of geological time, 2.5 Ga, 1.6 Ga, 1.0 Ga, c.539 Ma, c.252 Ma and c.66 Ma, sit within the downslope of troughs that follow peaks in zircon abundance. Note, however, that the time between the 'Nuna' peak at 1.87 Ga and the currently defined Paleoproterozoic-Mesoproterozoic boundary, which precedes a long-lived abundance trough, is anomalously long, and reflects protracted assembly of the Nuna supercontinent.

The effect of crustal processes on seawater composition is recorded by the $^{87}Sr/^{86}Sr$ ratios of marine carbonates. High $^{87}Sr/^{86}Sr$ values are attributed to times of increased exhumation of old radiogenic crystalline rocks that would accompany supercontinent amalgamation and disaggregation, while low $^{87}Sr/^{86}Sr$ values signify reduced exhumation of old crustal domains that occurs when

supercontinent breakup is accompanied by enhanced ocean ridge hydrothermal activity, rift-related magmatism and sea level rise (Veizer, 1989). Although commonly used seawater $^{87}Sr/^{86}Sr$ curves (Veizer et al., 1999; Shields and Veizer, 2002; Shields 2007) imply that continental weathering had little influence before the end of the Archean, recent studies (e.g. Satkoski et al., 2016) suggest that continental weathering and low-temperature surface alteration were more important than previously suspected during the Archean. Two prolonged peaks in the Sr isotope composition of seawater correspond with the Paleoproterozoic-Mesoproterozoic and Neoproterozoic-Phanerozoic transitions (Shields, 2007; Kuznetsov et al., 2018). These intervals of enhanced continental weathering of more radiogenic rocks coincide with the amalgamation of Nuna and Pannotia/Gondwana, respectively (e.g. Cawood et al., 2013; Nance and Murphy, 2018). The widespread orogenesis that accompanied amalgamation of Rodinia (Namaqua-Natal (Africa), Grenville-Sveconorwegian (North America-Europe) and Sunsás (South America) does not feature prominently in the seawater Sr isotope curve or zircon εHf compilations, likely because these orogens primarily involved juvenile arcs in external orogens (e.g. Spencer et al, 2013) rather than old radiogenic crustal domains. The dominant influence of lithology over weathering rates on the $^{87}Sr/^{86}Sr$ record is consistent with the observed negative covariation between $^{87}Sr/^{86}Sr$ and zircon εHf records (Hawkesworth et al., 2016).

Supercontinent amalgamation has been proposed to increase nutrient availability (including important bio-limiting nutrients such as iron and phosphorus, e.g. Tyrell, 1999) and organic production via higher rates of chemical weathering, leading to pulses of oxygenation (Campbell and Allen, 2008). However, the concept of greatly increased weathering rates would appear to be in conflict with the silicate weathering feedback, which regulates the long-term carbon cycle (Walker et al., 1981). Moreover, carbon isotope trends, which are commonly used to mirror changes in organic burial and therefore oxygenation (e.g. Des Marais et al., 1992; Lyons et al., 2014), may relate instead to tectonic forcing of carbonate weathering, resulting in an inverse (or no) covariation between $\delta^{13}C$ and carbon burial (Shields and Mills, 2017). The relationship between $\delta^{13}C$ excursions and oxygenation is made more complex when we consider that oxidative weathering of organic carbon could have been limited by low atmospheric oxygen (Bekker and Holland, 2012; Daines et al., 2017). As a consequence, negative as well as positive carbon isotope excursions could indicate Proterozoic oxygenation events, driven instead by pyrite burial, particularly at times of enhanced evaporite sulfate weathering since about 2.0 Ga (Shields et al., 2019). Despite the widespread acceptance of a two-step rise in atmospheric oxygen during the Proterozoic Eon (Lyons et al., 2014), sophisticated biogeochemical models have seldom been applied to the Precambrian Earth system and few proxies exist to constrain absolute atmospheric oxygen levels (Planavsky et al., 2014).

Geochemical evidence indicates that during much of the Proterozoic Eon, upper oceans were oxygenated due to mixing with the atmosphere, but the deep ocean in contrast still tended towards anoxia with local euxinia (Canfield, 1998; Shen et al., 2002; Arnold et al., 2004; Poulton et al., 2004; Farquhar et al., 2010). However, the extent of surface oxygenation is still highly disputed (Slack et al., 2007; Planavsky et al., 2014; Tang et al., 2016; Zhang et al., 2016; Daines et al., 2017). Deep ocean anoxia suggests that atmospheric oxygen levels were low enough that oxygen became easily exhausted at productive margins where organic remineralisation scavenged first oxygen then sulphate. After the assembly of Rodinia, euxinia became less common, leading to mostly ferruginous conditions (Guilbaud et al., 2015). Under such conditions efficient phosphorus removal may have helped to sustain low atmospheric oxygen levels (Guilbaud et al., 2020). A two-step oxygenation history (first surface oceans and atmosphere and then deep oceans) has also been supported by Fe speciation studies, which show increased amounts of Fe (III) relative to Fe (II) in subaerial volcanic rocks after the GOE, but no change in submarine volcanics until after the NOE (Stolper and Brenhin-Keller, 2018).

How environmental parameters, such as climate and redox conditions, were modulated by the supercontinent cycle remains uncertain but tectonic and environmental changes track the same episodicity, providing optimism that natural subdivision of the Proterozoic Eon would be geologically meaningful. Plume generated LIP magmatism could also help define natural Precambrian (and Phanerozoic) boundaries through their likely effects on the wider environment (Horton, 2015; Ernst and Youbi 2017; Ernst et al. 2020). Examples include the Archean-Siderian boundary LIPs (2460-2450 Ma Matachewan and coeval events in Karelia-Kola and Pilbara cratons), Rhyacian-Orosirian boundary LIPs (2058 Ma Bushveld and Kevitsa events), Orosirian-Statherian boundary (1790 Ma LIPs on many blocks), Statherian-Calymmian boundary (1590 Ma LIPs), Calymmian-Ectasian boundary (1385 Ma

LIPs on many cratons), Ectasian-Stenian boundary (c. 1205 Ma Marnda Moorn LIP), Stenian-Tonian boundary (c. 1005 Ma Sette Daban event or c. 925 Ma Dashigou event), Tonian-Cryogenian (720 Ma Franklin LIP and other related LIPs (Ernst and Youbi 2017). Despite the difficulty matching the isotopic record with LIP emplacement and weathering, the 720 Ma Tonian-Cryogenian boundary, now defined by the start of the Sturtian glaciation, has been linked to the Franklin Large Igneous Province (LIP) of northern Laurentia (Macdonald et al., 2010; Macdonald and Wordsworth, 2017; Ernst and Youbi, 2017) and potentially other LIP fragments (Ernst et al., 2020) either through an increase in planetary albedo associated with the release of aerosols or an increase in global weatherability associated with the tropical emplacement of soluble Ca- and Mg-rich flood basalts. This discovery builds on the recognition that LIPs are coeval with many Phanerozoic chronostratigraphic boundaries and that, although regional in scale, LIPs can have global environmental effects and leave global sedimentary records. Thus, while LIPs are not "golden spikes" in themselves, they can represent proxies for golden spikes in the sedimentary record, which bodes well for Proterozoic stratigraphic correlation along Phanerozoic lines.

There is a clear consensus that the Earth's surface environment evolved in a series of events that were controlled ultimately by magmatism and tectonics. In this, there appears to be no essential difference between major geological transitions of the Phanerozoic and Proterozoic, all of which reflect complex interactions and feedbacks between the lithosphere, atmosphere and biosphere. Despite significant gaps in understanding, various isotopic and geochemical proxies track tectonic (supercontinent) cyclicity and offer prospects for a more robust, rock-based pre-Cryogenian time scale.

4. Nascent potential of Proterozoic biostratigraphy and chemostratigraphy

Stromatolite textures (and structures) were once thought to be age-diagnostic, although this is now more frequently interpreted to reflect a general tendency towards greater biological control over calcium carbonate precipitation through time (Grotzinger, 1990; Arp et al., 2001; Riding, 2008). Coarse sparry texture (botryoidal fans and, microdigitate stromatolites, dendrites, isopachous laminites, and herringbone calcite) is common in Late Archaean-Mesoproterozoic carbonate systems. Although such textures have commonly been referred to as seafloor cement, they formed at the open sediment-water interface rather than as void-fills, unlike later calcite microspar cements, which peaked in the early Neoproterozoic (James et al., 1998), just as cyanobacterial sheaths began to be calcified, forming clotted, 'thrombolite' mounds of calcimicrobial fabric (Arp et al., 2001). Despite evident trends, few if any sharp temporal divisions can be identified in stromatolite type or microbially induced sedimentary structures (MISS). For example, abiotically controlled seafloor carbonate precipitation did not entirely disappear at the end of the Archean, while the first occurrence of fossilised bacteria (or stromatolites) cannot be used to date the evolutionary origins of cyanobacteria (Blank, 2013; Sánchez-Baracaldo et al., 2017; although see Ward et al., 2016), which from geochemical data ought to predate Neoarchean evidence of oxygenation (Farquhar et al., 2011; Riding et al., 2014). Supposedly age-diagnostic sedimentary textures, like stromatolite fabrics, have lost favour, while discoveries of new fossils each year continually resurrect the hope that Precambrian biostratigraphy will be a genuine possibility.

Although Precambrian paleontology is a relatively young field, with only belated acceptance of Ediacaran body fossils (Glaessner, 1962), tremendous advances have been made in recent years. Nevertheless, Precambrian biostratigraphy is still in its infancy with respect to fossil discovery and systematic description. It is not unusual, for example, for a new discovery to extend the stratigraphic range of fossil species by tens or even hundreds of millions of years. Macroscopic forms are too rare or simple to be of stratigraphic use, and while organic-walled microfossils are common in both fine-grained siliciclastic sedimentary rocks or concretions, assemblages are typically dominated by simple, smooth-walled vesicles known as *Leiosphaeridia*, a biologically uninformative acritarch taxon. Nonetheless, with a growing number of taxonomic studies linked to new paleoenvironmental, chemostratigraphic and geochronologic constraints (e.g., Sergeev et al., 2012; Tang et al., 2013, 2015; Baludikay et al., 2016; Porter and Riedman 2016; Riedman and Porter, 2016; Beghin et al. 2017a, b; Loron and Moczydłowska, 2017; Loron et al., 2019a; Cohen et al. 2017a,b; Javaux and Knoll, 2017; Miao et al., 2019), a nascent Proterozoic biostratigraphic record is beginning to take shape.

4.1 Biostratigraphy of the Proterozoic Eon (Eonothem)

The oldest macroscopic organic-walled fossils are known from Paleoproterozoic rocks (Han and Runnegar, 1992; Javaux and Lepot, 2018), now dated to <1891 ± 3 Ma (Pietrzak-Renaud and Davis, 2014). However, these simple coils and spirals, similar in appearance to *Grypania spiralis* (e.g., Walter et al., 1976; Sharma and Shukla, 2009), are not diagnostically eukaryotic in affinity. Decimeter-sized seaweed-like compressions (Zhu et al., 2016) and ornamented acritarchs occur in rocks at c. 1.6 Ga (e.g. Miao et al., 2019) and are widely considered to be the first convincing fossilised eukaryotes (Javaux and Lepot, 2018).

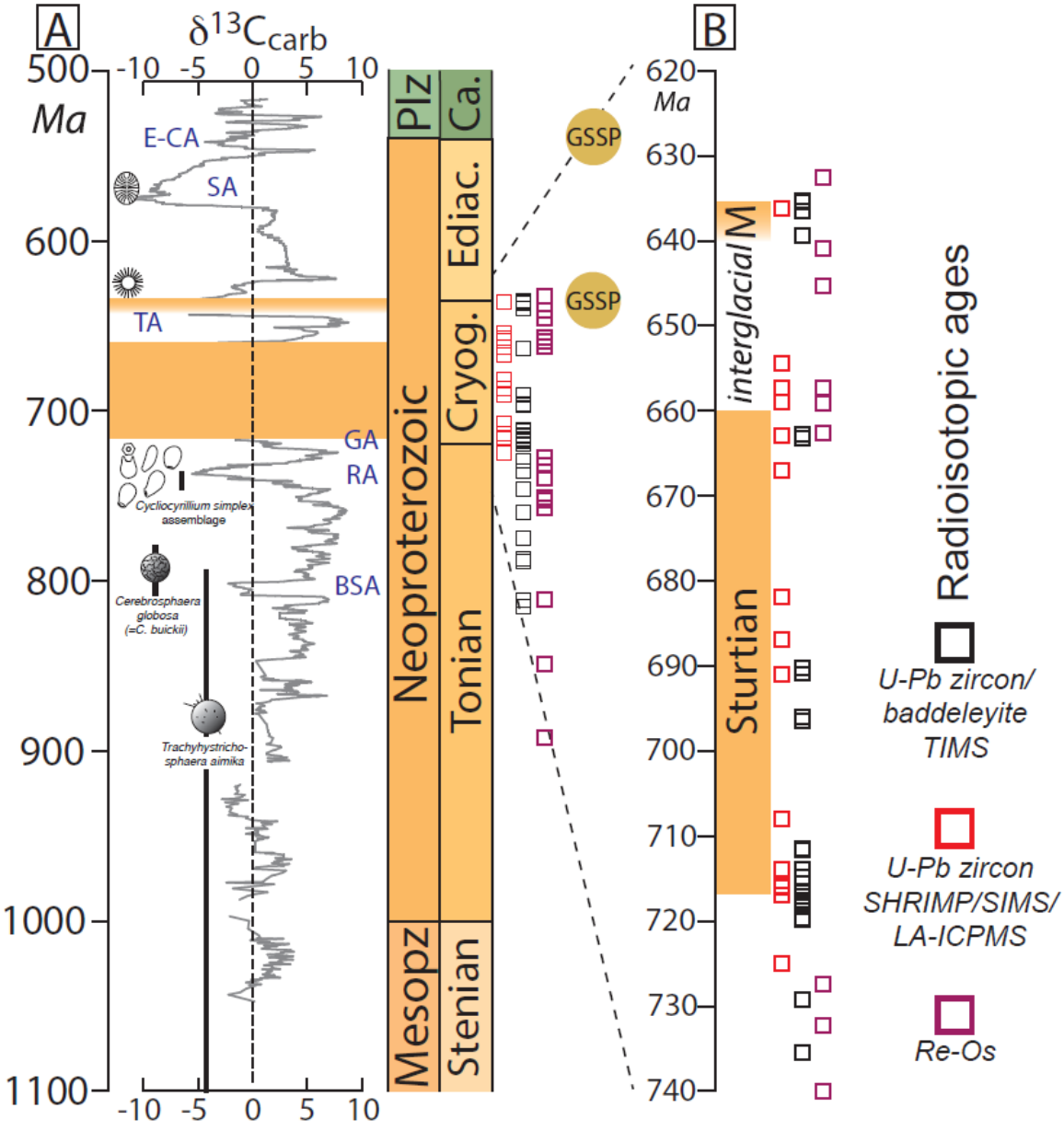

Fig. 4. *The Neoproterozoic geological time scale (after Halverson et al., 2020). Negative carbon isotope anomalies (BSA = Bitter Springs Anomaly; RA = Russøya anomaly; GA = Garvellach anomaly; TA = Trezona Anomaly; SA = Shuram Anomaly; E-CA = Ediacaran-Cambrian boundary anomaly). Minimum biostratigraphic ranges are also shown for* Trachyhystrichosphaera aimika*,* Cerebrosphaera globosa *(=*C. buickii*), and the* Cycliocyrillium simplex *assemblage. Geochronological age constraints for the Tonian and Cryogenian period (along with ages from the early Ediacaran Period that provide minima on*

the Cryogenian-Ediacaran boundary) are shown (in open squares) by type of age determination. B. Expanded view of the age constraints that establish the synchronous onset and end of the Cryogenian glaciations.

Molecular clock analyses place the origin of crown-group eukaryotes sometime in the Mesoproterozoic or late Paleoproterozoic (e.g., Berney and Pawlowski, 2006; Parfrey et al., 2011; Eme et al., 2014; Betts et al., 2018). Some phylogenetic data suggest that the first photosynthetic eukaryotes may have emerged in freshwater habitats (Blank, 2013; Sanchez-Baracaldo et al., 2017), which may lower their preservation potential in the rock record. The Stenian-Tonian transition interval is increasingly being viewed as a time of crown group eukaryote diversification (e.g. Knoll et al., 2006; Cohen and Macdonald, 2015; Butterfield, 2015; Xiao and Tang, 2018). Latest Mesoproterozoic and earliest Neoproterozoic rocks are the first to preserve fossils with clear similarities to particular modern eukaryotic clades, including red and green algae, fungi, amoebozoans, and stramenopiles (Butterfield et al., 1994; Butterfield, 2004; Porter et al., 2003; Nagovitsin, 2009; Loron et al., 2019b; Tang et al., 2020), though the affinities of most early Neoproterozoic fossils remain enigmatic. A number of eukaryotic innovations also appear in the record during this time, including scales, tests, biomineralization, and eukaryovory (Porter and Knoll, 2000; Cohen and Knoll, 2012; Cohen et al., 2017a,b; Porter, 2016). In addition, eukaryote-derived sterane biomarkers appear for the first time c. 810 Ma (Brocks, 2018; Zumberge et al., 2019).

Given these evolutionary changes, it is not surprising that late Mesoproterozoic/early Neoproterozoic fossil assemblages are largely distinct from those of early Mesoproterozoic age (Sergeev et al., 2017), and that several organic-walled microfossils have been proposed as index fossils for this interval. These include the acritarch *Trachyhystrichosphaera aimika* (spheroidal vesicles with sparse, irregularly distributed, hollow processes), which is found in more than 20 sections worldwide in Stenian and Tonian strata, aged c. 1100 to c. 800 Ma (Butterfield et al., 1994; Tang et al., 2013; Riedman and Sadler, 2018) or c. 1150 to c. 720 Ma (Pang et al., 2020) and *Cerebrosphaera globosa* (=*C. buickii*), robust spheroidal vesicles with distinctive wrinkles, common in late Tonian units c. 800–740 Ma (Hill et al., 2000; Grey et al., 2011; Riedman and Sadler, 2018) (Fig. 4).

Several other distinctive fossils from rocks c. 780–740 Ma have potential in subdividing the Tonian, but there are too few occurrences known at present to have confidence in their ranges (Riedman and Sadler, 2018). Vorob'eva et al. (2009) noted that many long-ranging early Neoproterozoic and late Mesoproterozoic taxa may be biostratigraphically useful with respect to their last appearances, and in this regard it is worth noting that Riedman and Sadler (2018) found that the disappearance of many ornamented taxa in the later Tonian occurred just before or around the time that the distinctive vase-shaped microfossils appear. The vase-shaped microfossils, constrained to range from c. 790-730 Ma (Riedman and Sadler, 2018; Riedman et al., 2018), provide the most promising biostratigraphic marker for subdividing Tonian time, and may be useful in defining the Cryogenian GSSP (Strauss et al., 2014), although it is not clear the extent to which the range is controlled by taphonomic factors.

4.2 Chemostratigraphy of the Proterozoic Eon (Eonothem)

With the possible exception of the Neoarchean, chemostratigraphy of the Precambrian is restricted to the Proterozoic Eon. The GOE can be traced using a number of redox-sensitive geochemical proxies, e.g. mass-independent fractionation of sulfur isotopes, trace metal concentrations and isotopes, while related changes to microbial metabolisms and biogeochemical cycles may be apparent in nitrogen, iron and other isotope records.

For later portions of the sedimentary archive, the carbon isotope record has most potential for identifying chemo-oceanographic events during the Proterozoic, beginning with the widespread positive anomaly (anomalies), referred to the Lomagund-Jatuli Event (LJE), which started before c. 2.22 Ga and ended by 2.06 Ga (Karhu and Holland, 1996; Melezhik et al., 2007; Martin et al., 2013). Later negative anomalies have been reported at about 2.0 Ga (Kump et al., 2011; Ouyang et al., 2020), 1.6 Ga (Zhang, K. et al., 2018; Kunzmann et al., 2019), 0.93 Ga (Park et al., 2016). Carbon and strontium isotope stratigraphy (mainly on marine carbonates) are the most widely applied chemostratigraphic tools in the Neoproterozoic, and notwithstanding challenges to their general robustness to diagenetic alteration (e.g., Knauth and Kennedy, 2009; Derry, 2010) and reliability as

global seawater proxies (Ahm et al., 2019), consistently reveal similar secular trends at both basinal and global scales.

The early Neoproterozoic carbon isotope record is identified by its sustained intervals of high $\delta^{13}C_{carb} \geq +5‰$ (Fig. 4; Kaufman et al., 1997; Halverson et al., 2005). The shift towards the high $\delta^{13}C_{carb}$ values appears to be transitional, with moderate fluctuations ($\leq 4‰$) in $\delta^{13}C_{carb}$ beginning in the late Mesoproterozoic (Knoll et al., 1995; Bartley et al., 2001; Kah et al., 2012) and continuing into the early Neoproterozoic (Kuznetsov et al., 2006). However, due to a paucity of earliest Neoproterozoic marine carbonate successions globally and poor age control on those successions that do exist, the $\delta^{13}C_{carb}$ record for the interval c. 1100–850 Ma is still poorly constrained. Available data indicate that significant $\delta^{13}C_{carb}$ excursions could have taken place during this interval but values remained between -5‰ and 5‰, while $^{87}Sr/^{86}Sr$ fluctuated between 0.7052 and 0.7063 (Fig. 5; Cox et al., 2016; Kuznetsov et al., 2017; Zhou et al., 2020).

The shift towards higher sustained $\delta^{13}C_{carb}$ ($\geq 5‰$) values occurred at c. 850 Ma (though not directly dated), as recorded in the Little Dal Group and equivalent strata of northwestern Canada (Fig. 5; Halverson, 2006; Macdonald et al., 2012; Thomson et al., 2015). However, this trend to high $\delta^{13}C_{carb}$ values is punctuated by a discrete and long-lived interval of near zero to negative $\delta^{13}C_{carb}$ values, referred to as the Bitter Springs Anomaly (BSA) (Halverson et al., 2005) after the Bitter Springs Formation in the Amadeus Basin of central Australia where it was first documented (Hill and Walter, 2000). The BSA is well documented in central Australia, Svalbard, northwestern Canada, Ethiopia (Swanson-Hysell et al., 2012, 2015; and references therein) and possibly India (George et al., 2018). It is constrained by U-Pb zircon CA-TIMS ages to have initiated after 811.5 Ma (Macdonald et al., 2010) and terminated prior to 788.7 Ma (MacLennan et al., 2018). Using a thermal subsidence-type age model applied to Svalbard, Halverson et al. (2018) estimated the BSA to have begun c. 810 Ma and ended c. 802 Ma, for a duration of 8 million years.

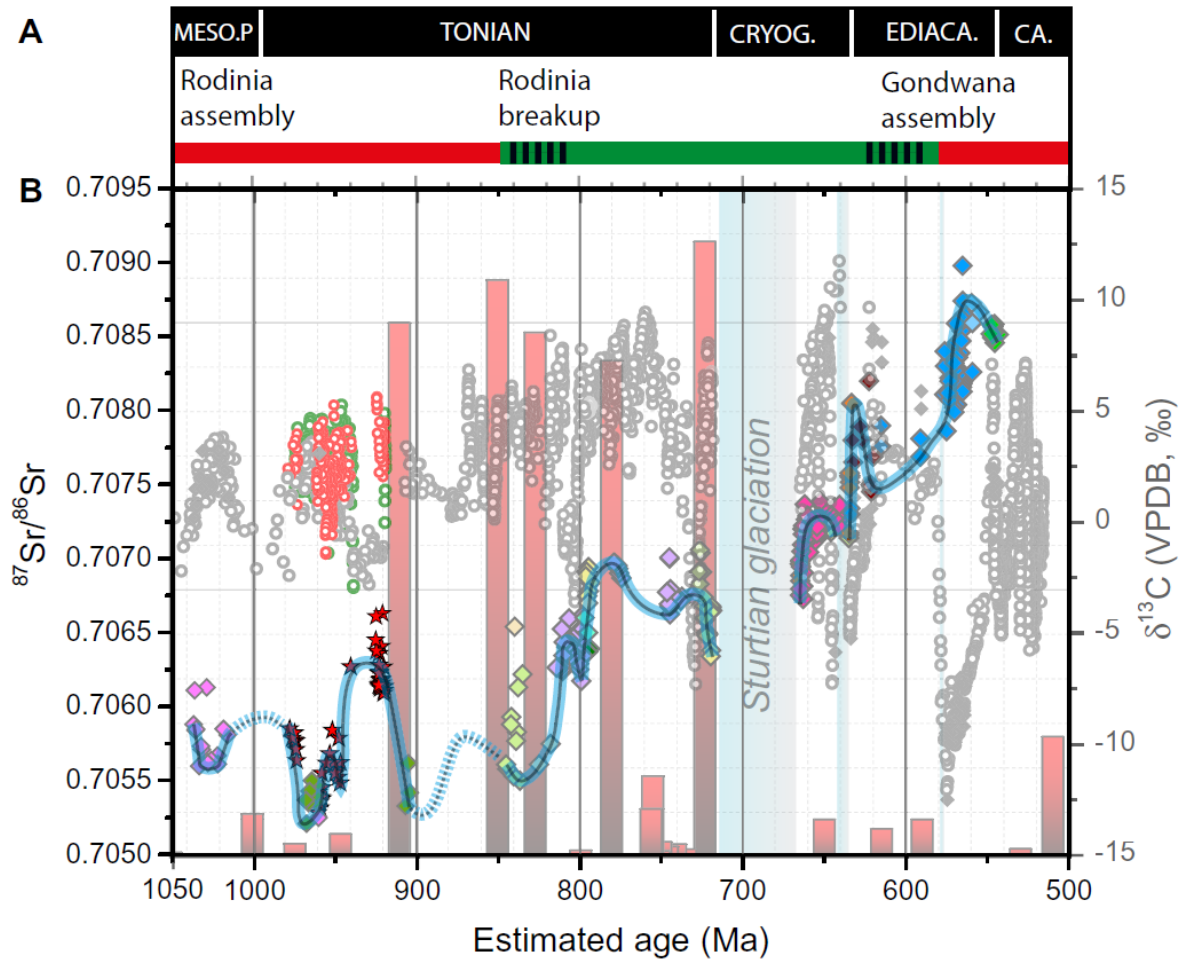

Fig. 5. *Neoproterozoic seawater strontium isotope curve (blue line) superimposed on known large igneous provinces (red bars) and the carbon isotope record (after Zhou et al., 2020).*

Available strontium isotope data show a plateau near 0.7070 following recovery from the Bitter Springs anomaly that is punctuated by a few minor downturns. A larger decline down to 0.7064–0.7065 broadly coincides with the recovery from the c. 738–735 Ma Russøya negative $\delta^{13}C_{carb}$ excursion (Halverson et al., 2018; MacLennan et al., 2018). Cox et al. (2016) suggested that these late Tonian declines in $^{87}Sr/^{86}Sr$ were driven by preferential silicate weathering of continental flood basalt associated with the breakup of Rodinia, with the larger late Tonian drop to 0.7064 corresponding to weathering of juvenile arcs in the Arabian-Nubian Sheild (Park et al., 2019). Furthermore, the early Neoproterozoic $^{87}Sr/^{86}Sr$ record is strongly biased by data from a small handful of successions (mainly Svalbard and NW Canada) and suffers from poor age control. Additional high-quality Sr isotope data are necessary to fill in the secular record of Neoproterozoic seawater $^{87}Sr/^{86}Sr$, and have been forthcoming from Russia (Kuznetsov et al., 2017) and the North China craton (Zhou et al., 2020).

The broad contours of the secular trend in Tonian–Cryogenian seawater $^{87}Sr/^{86}Sr$ are now well established, dominated by a long-term rise in $^{87}Sr/^{86}Sr$ (from ~0.7052 to ~0.7073; Fig. 5). However, strontium isotope chemostratigraphy in the Neoproterozoic is severely limited by the small number of stratigraphic intervals containing limestones that are sufficiently well preserved (i.e., with high Sr/Ca and low Mn/Sr) to record reliably the $^{87}Sr/^{86}Sr$ of contemporaneous seawater. Therefore, the record is constructed typically from small numbers of data points from discrete intervals in different successions. When combined with limited age control on most samples, the result is an irregular record with a large number of temporal gaps and limited verification of trends among coeval successions (Fig. 5). Moreover, due to the near absence of syn-glacial carbonate strata, no proxy data for seawater exist for the Cryogenian glacial intervals (i.e. c.717–660 and c.≥640–635.5 Ma). Nevertheless, due to the prominent rise in $^{87}Sr/^{86}Sr$ through the Neoproterozoic, the strontium isotopic record can potentially distinguish between the early Tonian (i.e., 1000–810 Ma), late Tonian (810–720 Ma) and Cryogenian non-glacial interval (c. 660–650 Ma).

5. Discussion

The embryonic nature of Proterozoic bio- and chemostratigraphy outlined above illustrates how ratification of pre-Cryogenian GSSPs lies far in the future and beyond the scope of the current review, which is focussed on a template for agreed rock-based criteria to permit the removal of current GSSAs, to be replaced by interim chronostratigraphic units, bounded by approximate ages. Development of a natural Precambrian time scale, especially for periods (systems), is still a 'work in progress' but we consider nevertheless that robust, rock-based subdivision is already possible, desirable and overdue. In working towards this aim, it is however important not to lose sight of the merits of the established chronometric scheme, which has served geologists well over the last 30 years. Indeed, it would appear that most boundaries would change by only small degrees. In order for future units of time (and strata) to be both widely acceptable and scientifically meaningful, they need to be fully defined conceptually, as has been done for the Cryogenian, Ediacaran and Cambrian periods, before they can be pinned down numerically.

As detailed above, the boundary definitions for the Hadean, Archean, Proterozoic and Phanerozoic eons help to broadly delimit four distinct parts of Earth history that are characterised by particular tectonic and biogeochemical regimes. Similarly, the eras of the Proterozoic Eon are recognised to be distinct intervals of tectonic, environmental and biological significance. The goal of any revision to the Precambrian geological time scale should therefore be to minimise disruption to both the current international time scale and existing regional and national stratigraphic norms. In this vein, it may be pertinent to recall the advice given by James (1978), following Trendall (1966), that: (1) "the classification should be the simplest possible that will meet immediate needs [as] every additional complexity provides a basis for disagreement or rejection; (2) The subdivision of time embodied in the classification should reflect major events in Earth's history, yet not be in such a form as to inhibit critical review of that history; (3) The classification must be acceptable to most students of the Precambrian; (4) The nomenclature should not be identified closely with one particular region; and (5) The subdivision scheme should be accompanied by operational criteria, so that assignment to the

classification will be guided by objective rather than theoretical considerations". It is in this spirit that we explore below how an improved rock-based geological time scale might depart from the existing chronometric time scale.

5.1 Tripartite rock-based subdivision of Archean time

The current geological time scale divides the Archean into four eras, although none of these eras (or the preceding Hadean Eon) has been formally defined or ratified. Successive studies of crustal evolution have tended to favour a simpler three-fold subdivision of the Archean even if the precise numerical boundaries of those eras differ in each study. We support a tripartite subdivision because the rationale for the Eoarchean is conceptually unsound as it seems to be based on the chance preservation of crustal fragments rather than on any fundamental change in Earth history. Although a rock-based onset for the Archean Eon at c. 3.85 Ga is supported by some (Bleeker, 2004; Kamber, 2015), proposing a specific age for the Hadean-Archean boundary lies outside the scope of the current discussion. Moreover it is also too difficult at present to propose a robust subdivision of Archean time based on diagnostic rock assemblages with the possible exception of the Neoarchean Era. We consider that three rock-based Archean eras of equal duration would consititute a robust subdivision to be characterised by the following rock types and geological processes, while acknowledging that future advances in knowledge may amend these preferences in the future:

Paleoarchean (c. 4.0 Ga – c. 3.5 Ga) Oldest crustal fragments of largely mafic composition, widespread TTG (Tonalite-Trondhjemite-Granodiorite) granitization; remnants of metamorphosed supracrustals.

Mesoarchean (c. 3.5 Ga – c. 3.0 Ga) Development of the subcontinental lithospheric mantle. Appearance of granite-greenstone terranes (coeval Pilbara and Barberton cratons with high-grade, polymetamorphic granite-gneiss complexes elsewhere. Widespread uncontroversial stromatolite and other microbial fabrics, largely submerged continents, pulses in TTG magmatism that become progressively more potassium-rich. The base of the Mesoarchean could potentially be chosen for the first appearance of granite-greenstone terranes.

Neoarchean (c. 3.0 Ga – c. 2.45/2.5 Ga) The Neoarchean witnessed a major pulse of (more felsic) crustal growth and the first platform covers on stable Archean cratons (Witwatersrand, Transvaal, Pongola Supergroups, South Africa; Mount Bruce Supergroup, Western Australia). Coeval "youngest" widespread granite-greenstone terranes (Kenoran, North America; Eastern Goldfields, Western Australia; Bulawayan, Zimbabwe); largest Superior-type BIFs in Earth history (Hammersley and Transvaal groups); initiation of a nascent form of plate tectonics; first passive margins; oldest large carbonate platforms; methanogenic C-isotope signatures in kerogen; and traces of free oxygen from c. 3.0 Ga. We propose that the Neoarchean should include a redefined c. 2.63-2.45 Ga Siderian Period**,** encompassing BIF deposition of the Hammersley Group and coeval Transvaal. There is also potential for additional, as yet unnamed periods from c. 2.78-2.63 Ga, encompassing the basalt-rich Fortescue and Ventersdorp groups and coeval youngest widespread granite-greenstone terranes; and c. 3.0-2.78 Ga encompassing the first platform covers (Witwatersrand and Pongola Groups). The base of the Neooarchean could potentially be chosen for the first appearance of carbonate platform covers.

5.2 Tripartite rock-based subdivision of Proterozoic time

The current three-fold subdivision of the Proterozoic Eon is broadly accepted with each era following prolonged orogenesis associated with the amalgamation of a supercontinent, marked by zircon abundance peaks at around 2.7-2.5 Ga, 1.90-1.85 Ga and 1.05-1.00 Ga, respectively. The Archean-Proterozoic boundary follows two major zircon abundance peaks associated with the amalgamation of the putative megacontinent Kenora (Kenorland). Rock-based characteristics of the three Proterozoic eras might include:

Paleoproterozoic (≤2.5 Ga to ≤1.8 Ga) Plate tectonic regime switch; new platform covers accompanied by onset of widespread (global?) glaciation, oxygenation of the atmosphere (crossing the threshold of disappearance of mass-independent S-isotope fractionation), first widespread sulfate evaporites,

putative rise in continental freeboard (rising seawater $^{87}Sr/^{86}Sr$), positive $\delta^{13}C$ excursions (LJE). Era ends with widespread orogenesis, interpreted to mark the assembly of Nuna.

Mesoproterozoic (≤ 1.8 Ga to ≤1.0 Ga) Widespread stable cratons and major platform covers, coeval with final amalgamation of Nuna. Incorporates thick stromatolitic carbonate systems, with megascopic organic-walled fronds, beads, discs and coils, first ornamented microscopic acritarchs, appearance of multicellular red and green algae; rare negative $\delta^{13}C$ excursions, widespread euxinia. Era ends with widespread orogenesis, interpreted to mark the assembly of Rodinia.

Neoproterozoic (≤1.0 Ga to c. 0.539 Ga) New platform covers, coeval with final amalgamation, tenure and break-up of Rodinia. Diversification of eukaryotic algae and metazoans, rising but unstable seawater $^{87}Sr/^{86}Sr$, high-amplitude $\delta^{13}C$ excursions (>8‰) and climate perturbations, episodic ocean oxygenation. Following a prolonged interval of worldwide glaciation (Snowball Earth) , the era ends with evolution of the unique Ediacaran multicellular biota, as well as widespread orogenesis, uplift and erosion throughout the late Ediacaran to early Cambrian interval.

5.3 Rock-based period subdivisions of the Proterozoic Eon

Existing period-level GSSAs could be replaced by approximate chronostratigraphic ages as has been done for the Cryogenian Period. The Proterozoic period names of Plumb (1991) are retained below, with the addition of the Oxygenian Period (van Kranendonk et al., 2012):

Paleoproterozoic Era (currently from 2.5 Ga, but interim boundary proposed at c. 2.45 Ga)

Oxygenian Period replaces the Siderian Period (currently 2500 Ma – 2300 Ma) after *Sideros* (= iron), named for the voluminous "Banded Iron Formations" (BIFs) deposited between c. 2.6 and c. 2.4 Ga, and peaking at c. 2.45 Ga. This period was marked by widespread glaciation and oxygenation.

Rhyacian Period (currently 2300 Ma – 2050 Ma) after *Rhyax* (= stream of lava), named for the "injection of layered complexes". The name 'Rhyacian' was coined specifically for the exceptional c. 2.054 Ga Bushveld Igneous Complex of South Africa. The period is a generally quiet interval in terms of basin formation and orogeny. 2.2 Ga marks the onset of increased magmatism globally (Spencer, 2018) with the major Bushveld LIP emplaced near the end of the period. The most characteristic feature of this period is arguably the widespread occurrence of very high $\delta^{13}C$ values in marine carbonate rocks (the Lomagundi-Jatuli Event).

Orosirian Period (currently 2050 Ma – 1800 Ma) after *Orosira* (= mountain range), named for a "global orogenic period". This period is characterised by widespread orogenic events, reflected in an exceptional zircon abundance peak (Fig. 3), and interpreted to mark the main assembly of Nuna. The period incorporates the appearance of the first macroscopic fossils.

Mesoproterozoic Era (to begin at or after c. 1.8 Ga)

Statherian Period (c. 1800 Ma – c. 1600 Ma) after *Statheros* (= stable), named for "stabilization of cratons". This period is characterized on most continents by new platforms and by coeval orogeny marginal to Nuna (e.g. North America; Kimban Orogeny, South Australia). The McArthur Basin of northern Australia represents a suitable candidate 'Stratotype'. The sandstone-volcanic Tawallah Group and Carson LIP, pass up into stromatolitic carbonates of the McArthur Group, encompassing the full interval from 1800 -1600 Ma with several age-constrained sequence breaks. Coeval sandstone-volcanic sequences in Brazil (Diamantina Group), central Africa (Chela Group), Russia (Lower Riphean), and north China (Changcheng Group) (north China).

Calymmian Period (c. 1600 Ma – c. 1400 Ma) after *Calymma* (= cover), named for "platform covers". This period is characterized by the expansion of existing platform covers. Microbially influenced

carbonates of the Jixian Group (North China) could provide a suitable 'Stratotype', although there are similar carbonate successions in coeval Lower Riphean (Russia). Final suturing of Nuna was followed by thick terrigenous basins; e.g, Roper Group (North Australia), Belt-Purcell Supergroups (North America), Paraguacu-Chapada Diamantina Groups (Brazil). The Statherian- Calymmian boundary is represented by a regional unconformity between the McArthur and Nathan Groups (McArthur Basin) in northern Australia.

Ectasian Period (c.1400 Ma – c. 1200 Ma) after *Ectasis* (= extension), named for "continued expansion of platform covers". A tectonically quiet period, with little basin development or orogeny; e.g., Xiamaling Group (North China), Yurmatau Grouip (Russia), Kibaran Supergroup (central Africa). Derim Derim-Yanliao and 1230 Ga Maojiagou LIPs. Little to distinguish it from the Calymmian Period, but retained for the present in Figure 6. No suitable "Stratotype" exists for now, although some authors have proposed a level close to the Jixian-Xiamaling group boundary, inferred to be c. 1400 Ma (between 1380 and 1440 Ma).

Stenian Period (c. 1200 Ma – c. 1000 Ma) after *Stenos* (= narrow), named for "narrow belts of intense metamorphism and deformation", e.g., Grenville, Musgrave, Sunsás, Namaqua orogenies. Conselheiro Mata Group (Brazil) and Keweenawan mafic rift (North America) elsewhere. Defining a chronostratigraphic from high-grade, deep crustal metamorphic rocks is problematic and specifically discouraged by ICS. An interim arbitrary base at c. 1200 Ma is assigned to encompass all the events across the "Grenvillian" belts, and coeval Conselheiro Mata Group.

Neoproterozoic Era (to begin at or after c. 1.0 Ga).

Tonian Period (currently 1000 Ma – c. 720 Ma) after *Tonas* (= stretch), named for the lithospheric stretching that we now associate with the breaking apart of the supercontinent Rodinia, now thought to have occurred largely after c. 800 Ma based on estimated rift lengths, evaporite deposits and flood basalts (Merdith et al., 2019). Although not currently essential, a new period might conceivably cover the preceding interval of cratonization from the final amalgamation to initial rupture of Rodinia, i.e. approximately ≤ 1.0 Ga to ≥0.8 Ga, with a revised Tonian Period from ≥0.8 Ga to c. 0.72 Ga. We tentatively propose the term 'Kratian' in figure 6, following *Kratos*, the Greek word for strength (cf. Statherian from *Statheros*).

6. Concluding remarks and recommendations

1) The four major divisions of Earth history are the Hadean, Archean, Proterozoic and Phanerozoic eons, whereby the Hadean-Archean boundary is taken to represent the start of the terrestrial rock record at c. 4.0 Ga.

2) Two first-order (*Archean and Proterozoic eon*) and six second-order (*Palaeoarchean, Mesoarchean, Neoarchean, Palaeoproterozoic, Mesoproterozoic, Neoproterozoic era*) stratigraphic intervals provide intuitive subdivision of post-Hadean / pre-Phanerozoic time. We consider that the Archean Eon would be more parsimoniously subdivided into three informal units of equal duration instead of the current four eras, to be defined further after detailed discussions by a commission of international experts.

3) Major transitions in Earth's tectonic, biological and environmental history occurred at approximately 2.5-2.3, 1.8-1.6 and 1.0-0.8 Ga. We consider, therefore, that current GSSAs at 2.5, 1.6 and 1.0 Ga could be replaced quite expeditiously by rock-based Proterozoic eras beginning at or after c. 2.5 Ga, c. 1.8 Ga and c. 1.0 Ga, respectively, based around these major transitions, all

of which occurred following orogenic peaks and during times of waning zircon abundance (post-acme, but not yet zenith) in line with Phanerozoic boundaries.

4) We suggest that current period-level GSSAs be replaced by improved rock-based concepts and interim chronostratigraphic units as soon as practicable, continuing recent progress towards that goal, illustrated, for example, by the establishment of an Ediacaran GSSP in 2004 and chronostratigraphic definition of the base of the Cryogenian at c. 720 Ma in 2012. Although all existing period names could be retained in a future chronostratigraphic scheme, some will need more conceptual underpinning, which would likely result in movement of the Siderian Period into the Archean Eon.

5) We recommend that a future Paleoproterozoic Era contain only three periods beginning (as now) at or after c. 2.5 Ga, c. 2.3 Ga and c. 2.05 Ga, respectively, so that the era begins near the end of major Archean BIF deposition, the onset of widespread glaciation and the Great Oxidation Event, but ends close to the onset of a prolonged period of cratonic, climatic and isotopic stability and first signs of eukaryotic life in the form of ornamented acritarchs and megascopic fronds. Future attention will likely focus on ensuring that rock-based Paleoproterozoic periods (currently Siderian, Rhyacian and Orosirian) bracket the natural phenomena for which they were named (BIF deposition, magmatism and orogenies, respectively). We propose that the Siderian Period be replaced by the Oxygenian Period (van Kranendonk et al., 2012; Fig. 6b) as the first period of the Paleoproterozoic Era.

6) We recommend that a future Mesoproterozoic Era contain four periods (Statherian at, or more likely after 1.8 Ga, Calymmian at c. 1.6 Ga, Ectasian at c. 1.4 Ga and Stenian at c. 1.2 Ga) so that it begins after major orogenies associated with Nuna amalgamation but before Statherian-age, putative eukaryote-grade fossil assemblages and ends after the Grenville orogeny near the time of the final amalgamation of Rodinia.

7) We recommend that a future Neoproterozoic Era contain three or four periods (a tentatively named, pre-Tonian *Kratian* period at or after c. 1.0 Ga, Tonian at c. 0.85 Ga, Cryogenian at c. 0.72 Ga and Ediacaran, which has a ratified GSSP) so that it begins around the final amalgamation of Rodinia and ends traditionally at the Ediacaran-Cambrian boundary.

8) These and further refinements of pre-Cryogenian time and strata could be proposed by new expert subcommissions to cover the 1) pre-Ediacaran Neoproterozoic (currently, the Cryogenian Subcommission), 2) Mesoproterozoic, 3) Paleoproterozoic and 4) Archean (+ Hadean).

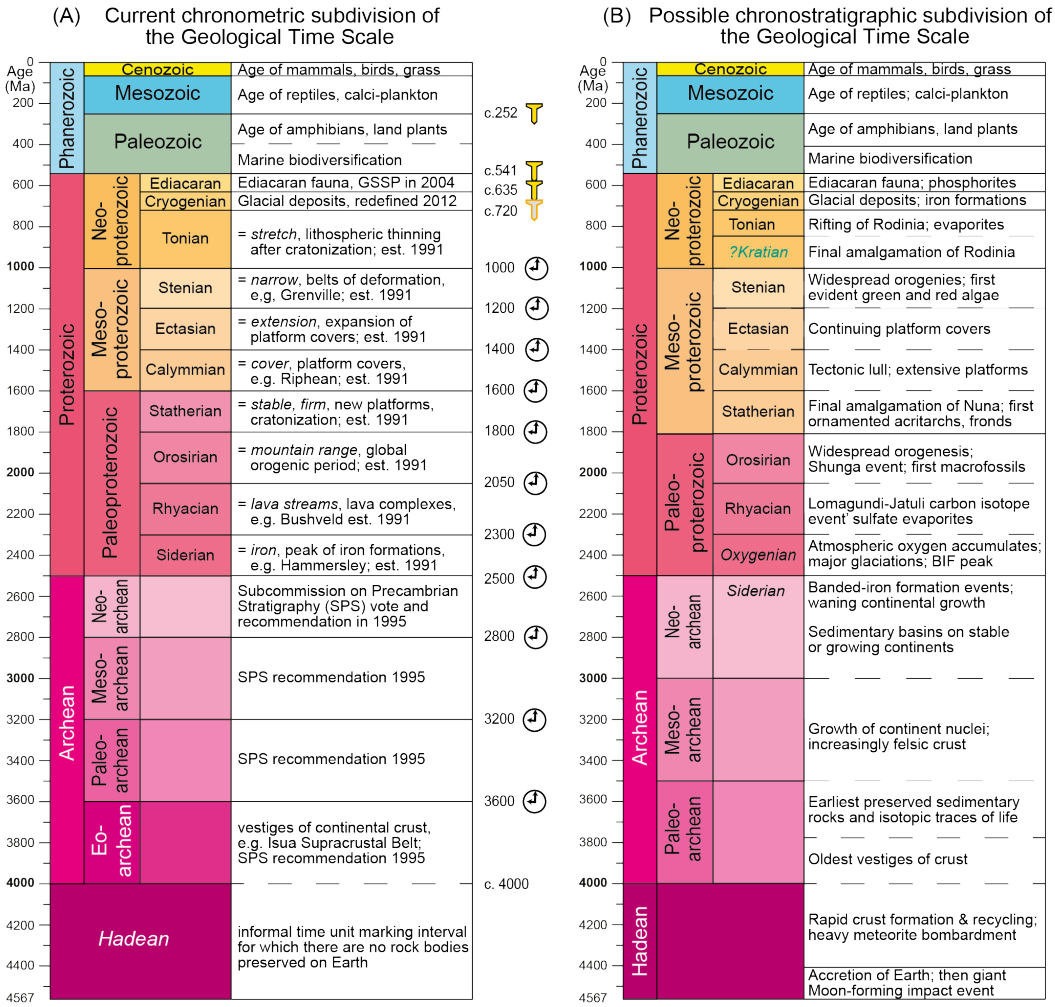

Fig. 6 *Proposed rock-based geologic time scale. Note that era and period boundary ages are approximate ages only and would inevitably change in any internationally agreed chronostratigraphic scheme. Period names in italics represent changes to existing nomenclature. If the first period of the Paleoproterozoic Era were named the 'Oxygenian' (van Kranendonk et al., 2012), we note that the term 'Siderian' would likely be retained for the final period of the Archean Eon. The name 'Kratian' is suggested to precede the Tonian as the first period of the Neoproterozoic Era.*

Acknowledgements

The authors are greatly indebted to the following for reading through drafts of the manuscript and for providing detailed critical analysis: A.K.Jain, Vivek Kale, Mihir Deb, M. Jayananda, Jyotiranjan Ray, Aivo Lepland, Peter Haines, Martin Whitehouse.

References

Adam, Z.R., Skidmore, M.L., Mogk, D.W., Butterfield, N.J., 2017. A Laurentian record of the earliest fossil eukaryotes. Geology 45, 387-390.

Ahm, A.-S. C., Maloof, A. C., Macdonald, F. A., Hoffman, P. F., Bjerrum, C. J., Bold, U., Rose, C. V., Strauss, J. V., Higgins, J. A., 2019. An early diagenetic deglacial origin for basal Ediacaran "cap dolostones". Earth and Planetary Science Letters 506, 292–307.

Alcott, L.J., Mills, B.J.W., Poulton, S.W., 2019. Stepwise Earth oxygenation is an inherent property of global biogeochemical cycling. Science, 6471, 1333-1337 doi: 10.1126/science.aax6459.

Anbar, A.D., Duan, Y., Lyons, T.W., Arnold, G.L., Kendall, B., Creaser, R.A., Kaufman, A.J., Gordon, G.W., Scott, C., Garvin, J., Buick, R., 2007. A whiff of oxygen before the Great Oxidation Event. Science, 317, 1903-1906.

Arnold, G. L., Anbar, A. D., Barling, J. and Lyons, T. W. 2004. Molybdenum isotope evidence for widespread anoxia in mid-Proterozoic oceans. Science, 304, 87–90.

Arp, G., Reimer, A., Reitner, J., 2001. Photosynthesis-induced biofilm calcification and calcium concentrations in Phanerozoic oceans. Science, 292, 1701-1074.

Ashwal, L.D., Bybee, G.M., 2017. Crustal Evolution and the temporality of anorthosites. Earth Science Reviews 173: 307-330.

Baludikay, B.K., Storme, J.Y., François, C., Baudet, D., Javaux, E.J., 2016. A diverse and exquisitely preserved organic-walled microfossil assemblage from the Meso–Neoproterozoic Mbuji-Mayi Supergroup (Democratic Republic of Congo) and implications for Proterozoic biostratigraphy. Precambrian Research 281, 166–184.

Bartley, J.K., Semikhatov, M.A., Kaufman, A.J., Knoll, A.H., Pope, M.C., Jacobsen, S.B., 2001. Global events across the Mesoproterozoic–Neoproterozoic boundary: C and Sr isotopic evidence from Siberia. Precambrian Research 111, 165–202.

Bédard, J.H., 2018. Stagnant lids and mantle overturns: Implications for Archean tectonics, magmagenesis, crustal growth, mantle evolution, and the start of plate tectonics. Geoscience Frontiers, 9, 19-49.

Beghin, J., Guilbaud, R., Poulton, S.W., Gueneli, N., Brocks, J.J., Storme, J.-Y., Blanpied, C., Javaux, E.J., 2017a. A palaeoecological model for the late Mesoproterozoic – early Neoproterozoic Atar/El Mreïti Group, Taoudeni Basin, Mauritania, northwesternAfric. Precambrian Research 299, 1–14.

Beghin, J., Storme, J.-Y., Blanpied, C., Gueneli, N., Brocks, J.J., Poulton, S.W., Javaux, E.J., 2017b. Microfossils from the late Mesoproterozoic – early Neoproterozoic Atar/El Mreïti Group, Taoudeni Basin, Mauritania, northwesternAfric. Precambrian Research 291, 63–82.

Bekker, A., 2014. Great Oxygenation Event. In: Encyclopedia of Astrobiology (eds: R. Amils et al.), Springer-Verlag, Berlin, Heidelberg, pp. 1-9.

Bekker, A., Holland, H.D., 2012. Oxygen overshoot and recovery during the early Paleoproterozoic. Earth and Planetary Science Letters, 317, 295-304.

Bekker, A, Holland, H.D, Wang, P.L., Ruble, D., Stein, H.J., Hannah, J.L., Coetzee, L.L., Beukes, N.J., 2004. Dating the rise of atmospheric oxygen. Nature, 427, 117-120.

Bekker, A., Karhu, J.A., Eriksson, K.A., Kaufman, A.J., 2003. Chemostratigraphy of Paleoproterozoic carbonate successions of the Wyoming Craton: tectonic forcing of biogeochemical change? Precambrian Research, 120: 279-325.

Bekker, A., Kaufman, A.J., 2007. Oxidative forcing of global climate change: a biogeochemical record across the oldest Paleoproterozoic ice age in North America. Earth and Planetary Science Letters, 258, 486-499.

Bekker, A., Planavsky, N., Rasmussen, B., Krapez, B., Hofmann, A., Slack, J.F., Rouxel, O.J., Konhauser, K.O., Iron formations: Their origins and implications for ancient seawater chemistry. Treatise on Geochemistry, 12, 561-628.

Bekker, A., Slack, J.F., Planavsky, N., Krapez, B., Hofmann, A., Konhauser, K.O., Rouxel, O.J., 2010. Iron formation: the sedimentary product of a complex interplay among mantle, tectonic, oceanic, and biospheric processes. Economic Geology, 105, 467-508.

Bengtson, S., Sallstedt T., Belivanova V., Whitehouse M., 2017. Three-dimensional preservation of cellular and subcellular structures suggests 1.6 billion-year-old crown-group red algae. PLoS Biol 15(3):e2000735.doi:10.1371/ journal.pbio.2000735.

Berney, C., Pawlowski, J., 2006. A molecular time-scale for eukaryote evolution recalibrated with the continuous microfossil record. Proceedings of the Royal Society B 273, 1867–1872.

Betts, H.C., Puttick, M.N., Clark, J.W., Williams, T.A., Donoghue, P.C.J., Pisani, D., 2018. Integrated genomic and fossil evidence illuminates life's early evolution and eukaryote origin. Nature Ecology & Evolution 2, 1556–1562.

Blank, C.E., 2013. Origin and early evolution of photosynthetic eukaryotes in freshwater environments: reinterpreting Proterozoic paleobiology and biogeochemical processes in light of trait evolution. Journal of Phycology, 49(6), 1040-1055.

Blättler, C.L., Claire, M.W., Prave, A.R., Kirsimäe, K., Higgins, J.A., Medvedev, P.V., 2018. Two-billion-year-old evaporites capture Earth's great oxidation. Science, 360: 320-323.

Bleeker, W., 2003. The late Archean record: a puzzle in c. 35 pieces. Lithos, 71: 99-134.

Bleeker, W., 2004. Towards a "natural" Precambrian time scale. In: Gradstein, F.M., Ogg, J.G., Smith, A.G. (Eds.), A Geologic Time Scale 2004. Cambridge University Press, Cambridge, pp. 141-146.

Bodorkos, S., Crowley, J.L., Claoue-Long, J.C., Anderson, J.R., Magee, C.W. Jr., 2020. Precise U-Pb baddelyite dating of the Derim Derim dolerite, McArthur Basin, Northern Territory: old and new SHRIMP and ID-TIMS constraints. Australian Journal of Earth Sciences, doi:10.1080/08120099.2020.1749929.

Bowring, S. A., Grotzinger, J. P., 1992. Implications of new chronostratigraphy for tectonic evolution of Wopmay orogen, northwest Canadian Shield. American Journal of Science, 292, 1-20.

Bowring, S.A., Williams, I.S., 1999. Priscoan (4.00–4.03 Ga) orthogneisses from northwestern, Canada. Contributions Mineralogy and Petrology, 134, 3–16.

Bradley, D. C., 2008. Passive margins through earth history. Earth-Science Reviews, 91, 1–26.

Brasier, M., Cowie, J., Taylor, M., 1994. Decision on the Precambrian-Cambrian boundary stratotype. Episodes, 17, 3-8.

Brasier, A.T., Fallick, A.E., Prave, A.R., Melezhik, V.A., Lepland, A., FAR-DEEP scientists, 2011. Coastal sabkha dolomites and calcitised sulphates preserving the Lomagundi-Jatuli carbon isotope signal. Precambrian Research, 189, 193-211.

Brasier, A.T., Martin, A.P., Melezhik, V.A., Prave, A.R., Condon, D.J., Fallick, A.E., 2013. Earth's earliest global glaciation? Carbonate geochemistry and geochronology of the Polisarka Sedimentary Formation, Kola Peninsula, Russia. Precambrian Research, 235, 278-294.

Brocks, J.J., 2018. The transition from a cyanobacterial to algal world and the emergence of animals. Emerging Topics in Life Sciences 2, 181–190.

Bull, S., Selley, D., Broughton, D., Hitzman, M., Cailteux, J., Large, R., McGoldrick, P., 2011. Sequence and carbon isotopic stratigraphy of the Neoproterozoic Roan Group strata of the Zambian copperbelt. Precambrian Research 190, 70–89.

Butterfield, N.J., 2000. Bangiomorphapubescens n. gen., n. sp.: implications for the evolution of sex, multicellularity, and the Mesoproterozoic radiation of eukaryotes. Paleobiology, 26, 386-404.

Butterfield, N.J., 2004. A vaucheriacean alga from the middle Neoproterozoic of Spitsbergen: implications for the evolution of Proterozoic eukaryotes and the Cambrian explosion. Paleobiology, 30, 231–252.

Butterfield, N.J., 2015. Early evolution of the Eukaryota. Palaeontology, 58, 5–17.

Butterfield, N.J., Knoll, A.H., Swett, K., 1994. Paleobiology of the Neoproterozoic Svanbergfjellet Formation, Spitsbergen. Fossils and Strata, 34, 1–84.

Campbell, I.H., Allen, C.A., 2008. Formation of supercontinents linked to increases in atmospheric oxygen. Nature Geoscience, 1, 554-558.

Canfield, D.E., 1998. A new model for Proterozoic ocean chemistry. Nature, 396, 450–453.

Canfield, D.E., Zhang, S., Wang, H., Wang, X., Zhao, W., Su, J., Bjerrum, C.J., Haxen, E.R., Hammarlund, E.U., 2018. A Mesoproterozoic iron formation. PNAS, doi:10.1073/pnas.1720529115.

Cawood, P.A., Hawkesworth, C.J., 2014. Earth's middle age. Geology, 42, 503-506.

Cawood, P.A., Hawkesworth, C.J., Dhuime, B. 2013. The continental record and the generation of continental crust. Geological Society of America Bulletin 125: 14-32.

Cawood, P.A., Hawkesworth, C.J., Pisarevsky, S.A., Dhuime, B., Capitanio, F.A., Nebel, O., 2018. Geological archive of the Onset of Plate Tectonics. Philosophical Transactions of the Royal Society A, 376, 20170405.

Chakraborty, P.P., Mukhopadhyay, J., Paul, P., Banerjee, D.M., Bera, M.K., 2020. Early atmosphere and hydrosphere oxygenation: Clues from Precambrian paleosols and chemical sedimentary records of India. Episodes, 43, 175-186.

Chemale, F., Dussin, I.A., Alkmim, F.F., Martins, M.S., Queiroga, G., Armstrong, R., Santos, M.N., 2012. Unravelling a Proterozoic basin history through detrital zircon geochronology: The case of the Espinhaço Supergroup, Minas Gerais, Brazil. Gondwana Research 22, 200-206.

Cloud, P., 1972. A working model of the primitive Earth. American Journal of Science, 272: 537-548.

Cloud, P., 1976. Major features of crustal evolution. Geol. Soc. South Africa, Alex L. Du Toit Mem. Lect. Ser., 14, 33pp.

Cloud, P., Glaessner, M.F., 1982. The Ediacarian Period and System: Metazoa inherit the Earth. Science 217, 783–792.

Cohen, P.A., Knoll, A.H., 2012. Scale Microfossils from the Mid-Neoproterozoic Fifteenmile Group, Yukon Territory. Journal of Paleontology 86, 775–800.

Cohen, P.A., Macdonald, F.A., 2015. The Proterozoic record of eukaryotes. Paleobiology 41, 610-632.

Cohen, P.A., Irvine, S.W., Strauss, J.V., 2017a. Vase-shaped microfossils from the TonianCallison Lake Formation of Yukon, Canada: taxonomy, taphonomy and stratigraphic palaeobiology. Palaeontology 60, 683–701.

Cohen, P. A., Strauss, J. V., Rooney, A. D., Sharma, M., Tosca, N., 2017b. Controlled hydroxyapatite biomineralization in an 810 million-year-old unicellular eukaryote. Science Advances 3, e1700095.

Condie, K. C., 1998. Episodic continental growth and supercontinents: a mantle avalanche connection? Earth and Planetary Science Letters 163, 97–108.

Condie, K.C., 2004. Supercontinents and superplume events: distinguishing signals in the geologic record. Physics of the Earth and Planetary Interiors, 146, 319–332.

Condie, K.C., 2014. Growth of continental crust: a balance between preservation and recycling. Mineralogical Magazine 78, 623–637.

Condie, K.C., Aster, R.C., 2010. Episodic zircon age spectra of orogenic granitoids: the supercontinent connection and continental growth. Precambrian Research, 180: 227-236.

Condie, K.C., O'Neill, C. Aster, R.C., 2009. Evidence and implications for a widespread magmatic shutdown for 250 Myr on Earth. Earth and Planetary Science Letters, 282, 294-298.

Condie, K.C., Puetz, S.J., 2019. Time series analysis of mantle cycles II: The geologic record in zircons, large igneous provinces and mantle lithosphere. Geoscience Frontiers, 10, 1327-1336.

Condon, D., Zhu, M., Bowring, S., Jin, Y., Wang, W., Yang, A., 2005. From the Marinoan glaciation to the oldest bilaterians: U-Pb ages from the Doushantuo Formation, China. Science 308, 95–98.

Cornell, D.H., Thomas, R.J., Gibson, R., Moen, H.F.G., Moore, J.M., Reid, D.L., 2006. Namaqua-Natal Province. In: Johnson, M.R., Anhauesser, C.R., Thomas, R.J. (Eds.), The Geology of South Africa. Geol. Soc. S. Afr, Johannesburg/Council for Geoscience, Pretoria, pp. 325–379.

Cox, G. M., Halverson, G. P., Stevenson, R. K., Vokaty, M., Poirier, A., Kunzmann, M., Li, Z.-X.,
Denyszyn, S. W., Strauss, J. V., Macdonald, F. A., 2016. Continental flood basalt weathering as a
trigger for Neoproterozoic Snowball Earth. Earth and Planetary Science Letters 446, 89–99.

Cox, G.M., Isakson, V., Hoffman, P.F., Gernon, T.M., Schmitz, M.D., Shahin, S., Collins, A.S., Preiss, W., Blades, M.L., Mitchell, R.N., Nordsvan, A., 2018. South Australian U-Pb zircon (CA-ID-TIMS) age supports globally synchronous Sturtian deglaciation. Precambrian Research 315, 257–263.

Crockford, P.W., Hodgskiss, M.S.W., Uhlein, G.J., Caxito, F., Hayles, J.A., Halverson, G.P., 2018. Linking paleocontinents through $\Delta^{17}O$ anomalies. Geology 46, 179–182.

Crosby, C.H., Bailey, J.V., Sharma, M., 2014. Fossil evidence of iron-oxidizing chemolithotrophy linked to phosphogenesis in the wake of the Great Oxidation Event. Geology 42, 1015-1018.

Crook, K.A.W., 1989. Why the Precambrian time-scale should be chronostratigraphic: A response to recommendations by the Subcommission on Precambrian stratigraphy. Precambrian Research, 43, 143-150.

Darling, J. R., Moser, D. E., Heaman, L. M., Davis, W. J., O'Neil, J., Carlson, R. (2014). Eoarchean to Neoarchean evolution of the Nuvvuagittuq Supracrustal belt: New insights from U-Pb zircon geochronology. American Journal of Science, 313(9), 844–876.

Daines, S.J., Mills, B.J.W., Lenton, T.M., 2017. Atmospheric oxygen regulation at low Proterozoic levels by incomplete oxidative weathering of sedimentary organic carbon. Nature Communications, 8, 14379, doi: 10.1038/ncomms14379.

Dana, J.D. (1872) American Journal of Science and Arts. 3rd series, **3**, 16, 250–257.

Derry, L.A., 2010. A burial diagenesis origin for the Ediacaran Shuram-Wonoka carbon isotope anomaly, Earth and Planetary Science Letters 292, 152–172.

Des Marais, D.J., Strauss, H., Summons, R.E., Hayes, J.M., 1992. Carbon isotope evidence for the stepwise oxygenation of the Proterozoic environment. Nature, 359, 605-609.

Domagal-Goldman, S.D., Kasting, J.F., Johnston, D.T., Farquhar, J., 2008. Organic haze, glaciations and multiple sulfur isotopes in the Mid-Archean Era. Earth and Planetary Science Letters, 269(1-2), pp.29-40.

Dunn, P.R., Plumb, K.A., Roberts, H.G., 1966. A proposal for time-stratigraphic classification of the Australian Precambrian. Geol. Soc. Aust. J., 13, 593-608.

Dunn, P., Thomson, B., Rankama, K., 1971. Late Pre-Cambrian glaciation in Australia as a stratigraphic boundary. Nature 231, 498–502.

Eme, L., Sharpe, S.C., Brown, M.W., Roger, A.J., 2014. On the age of eukaryotes: evaluating evidence from fossils and molecular clocks. Cold Spring Harbor Perspectives in Biology 6, a016139.

Ernst, R.E. and Youbi, N., 2017. How large igneous provinces affect global climate, sometimes cause mass extinctions, and represent natural markers in the geological record. Palaeogeography, Palaeoclimatology, Palaeoecology, 478, 30-52.

Ernst, R.E., Wingate, M.T.D., Buchan, K.L., Li, Z.-X. 2008. Global record of 1600–700 Ma Large Igneous Provinces (LIPs): Implications for the reconstruction of the proposed Nuna (Columbia) and Rodinia supercontinents. Precambrian Research 160, 159–178.

Ernst et al., 2020. Large Igneous Provinces. From: F.M. Gradstein, J.G. Ogg, M. Schmitz, G. Ogg. The Geologic Time Scale 2020. Elsevier Science Limited, in press.

Etienne, J.L., Allen, P.A., Rieu, R., Le Guerroué, E., 2007. Neoproterozoic glaciated basins: a critical review of the Snowball Earth hypothesis by comparison with Phanerozoic basins, in: Hambrey, M.J., Christoffersen, P., Glasser, N.F., Hubbard, B. (Eds.), Glacial Sedimentary Processes and Products. Volume 39 of International Association of Sedimentologists Special Publication, pp. 343–399.

Evans, D.A.D., Beukes, N.J., Kirschvink, J.L., 1997. A Paleoproterozoic Snowball Earth. Nature, 386, 262-266.

Evans, D.A.D., Mitchell, R.N., 2011. Assembly and breakup of the core of Paleoproterozoic-Mesoproterozoic supercontinent Nuna. Geology, 39, 443-446.

Evans, D.A.D., Trindade, R.I.F., Catelani, E.L., D-Agrella-Filho, M.S., Heaman, L.M., Oliveira, E.P., Soderlund, U., Ernst, R.E., Smirnov, A.V., Salminen, J.M., 2016. Return to Rodinia? Moderate to high palaeolatitude of the São Francisco / Congo craton at 920 Ma. From: Z. Li, D.A.D. Evans, J.B. Murphy (eds) Supercontinent Cycles Through Earth History, Geological Society, London, Special Publications, 424, 167-190.

Fairchild, I.J., Kennedy, M.J., 2007. Neoproterozoic glaciation in the Earth system. Journal of the Geological Society, London 164, 895–921.

Fareeduddin, Banerjee, D.M., 2020. Aravalli craton and its mobile belts: An update. Episodes, 43, 88-108.

Farquhar, J., Bao, H., Thiemens, M., 2000. Atmospheric influence of Earth's earliest sulphur cycle. Science, 289, 756-758.

Farquhar, J., Nanping, W., Canfield, D.E., Oduro, H., 2010. Connections between Sulfur Cycle Evolution, Sulfur Isotopes, Sediments, and Base Metal Sulfide Deposits. Economic Geology 105: 509-533.

Farquhar, J., Peters, M., Johnston, D.T., Strauss, H., Masterson, A., Wiechert, U. and Kaufman, A.J., 2007. Isotopic evidence for Mesoarchaean anoxia and changing atmospheric sulphur chemistry. Nature, 449, 706-709.

Farquhar, J., Zerkle, A.L., Bekker, A., 2011. Geological constraints on the origin of oxygenic photosynthesis. Photosynthesis Research, 107, 11-36.

Frimmel, H.E., 2005. Archaean atmospheric evolution: evidence from the Witwatersrand gold fields, South Africa. Earth Science Reviews 70, 1-46.

Frimmel, H.E., 2018. Episodic concentration of gold to ore grade through Earth's history. Earth Science Reviews 180, 148-158.

Gallagher, M., Whitehouse, M.J., Kamber, B.S., 2017. The Neoarchaean surficial sulphur cycle: An alternative hypothesis based on analogies with 20th-century atmospheric lead. Geobiology, 15, 385-400.

George, B.G., Ray, J.S., Shukla, A.D., Chatterjee, A., Awasthi, N. Laskar, A.H., 2018. Stratigraphy and geochemistry of the Balwan Limestone, Vindhyan Supergroup, India: Evidence for the Bitter Springs $\delta^{13}C$ anomaly. Precambrian Research, 313, 18-30.

Gibson, T.M., Wörndle, S., Crockford, P.W., Bui, T.H., Creaser, R.A., Halverson, G.P., 2019. Radiogenic isotope chemostratigraphy reveals marine and nonmarine depositional environments in the late Mesoproterozoic Borden Basin, Arctic Canada. Geological Society of America Bulletin, 131(11-12), 1965-1978, doi: 10.1130/B35060.1.

Gibson, G.M., Champion, D.C., Huston, D.L., Withnall, I.W., 2020. Orogenesis in Paleo-Mesoproterozoic Eastern Australia: A response to arc-continent and continent-continent collision during assembly of the Nuna supercontinent. Tectonics, doi: 10.1029/2019TC005717

Glaessner, M.F., 1962. Pre-Cambrian fossils. Biological Reviews, 37, 467-494.

Goldich, S.S., 1968. Geochronology in the Lake Superior region. Canadian Journal of Earth Science, 5, 715-724.

Grenholm, M., Schersten, A., 2015. A hypothesis for Proterozoic-Phanerozoic supercontinent cyclicity, with implications for mantle convection, plate tectonics and Earth system evolution. Tectonophysics, 662, 434-453.

Grey, K., Hill, A.C., Calver, C., 2011. Biostratigraphy and stratigraphic subdivision of Cryogenian successions of Australia in a global context. In: E. Arnaud, G.P. Halverson and G. Shields-Zhou (Editors), The Geological Record of Neoproterozoic Glaciations. Geological Society, London, Memoirs, 36, pp. 113–134.

Griffin, W.L., Belousova, E.A., O'Neill, C., O'Reilly, S.Y., Malkovets, V., Pearson, N.J., Spetsius, S., Wilde, S.A., 2014. The world turns over: Hadean-Archean crust-mantle evolution. Lithos, 189, 2-15.

Grotzinger, J.P., 1990. Geochemical model for Proterozoic stromatolite decline. Am. J. Sci., 290-A, 80–103.

Guadagnin, F., Chemale Jr., F., Magalhães, J., Santana, A., Dussin, I., Takehara, L., 2015. Age constraints on crystal-tuff from the Espinhaço Supergroup - insight into the Paleoproterozoic to Mesoproterozoic intracratonic basin cycles of the Congo-São Francisco Craton. Gondwana Research 27, 363-376.

Guilbaud, R., Poulton, S.W., Butterfield, N.J., Zhu, M., Shields, G.A., 2015. A global transition into ferruginous conditions in the early Neoproterozoic oceans. Nature Geoscience, 8(6), 466-470 doi:10.1038/NGEO2434.

Guo, Q., Strauss, H., Kaufman, A.J., Schroder, S., Gutzmer, J., Wing, B., Baker, M.A., Bekker, A., Jin, Q., Kim, S., Farquhar, J., 2009. Reconstructing Earth's surface oxidation across the Archean-Proterozoic transition. Geology, 37, 399-402.

Guitreau, M., Blichert-Toft, J., Mojzsis, S. J., Roth, A. S. G., & Bourdon, B., 2013. A legacy of Hadean silicate differentiation inferred from Hf isotopes in Eoarchean rocks of the Nuvvuagittuq supracrustal belt (Québec, Canada). Earth and Planetary Science Letters, 362, 171–181.

Gumsley, A.P., Chamberlain, K.R., Bleeker, W., Söderlund, U., de Kock, M.O., Larsson, E.R., Bekker, A., 2017. Timing and tempo of the Great Oxidation Event. PNAS, 114: 1811-1816,

Halevy, I., Johnston, D.T., Schrag, D.P., 2010. Explaining the structure of the Archean mass-independent sulfur isotope record. Science 329, 204-207.

Halverson, G.P., 2006. A Neoproterozoic chronology. In: Xiao, S., Kaufman, A. (Eds.), Neoproterozoic Geobiology and Paleobiology. Vol. 27 of Topics in Geobiology. Springer, Dordrecht, the Netherlands, pp. 231–271.

Halverson, G.P., Hoffman, P.F., Schrag, D.P., Maloof, A.C., Rice, A.H., 2005. Towards a Neoproterozoic composite carbon isotope record. Geological Society of America Bulletin 117, 1181–1207.

Halverson, G. P., Kunzmann, M., Strauss, J. V., Maloof, A. C., 2018. The Tonian-Cryogenian transition in Svalbard. Precambrian Research 319, 79–95.

Halverson, G.P., Porter, S.M., Shields, G.A. (2020) The Tonian and Cryogenian periods. From: F.M. Gradstein, J.G. Ogg, M. Schmitz, G. Ogg). The Geologic Time Scale 2020. Elsevier Science Limited, in press.

Han, T., Runnegar, B., 1992. Megascopic eukaryotic algae from the 2.1-billion-year-old Negaunee Iron-Formation, Michigan. Science 257:232–235.

Hardisty, D.S., Lu, Z., Bekker, A., Diamond, C.W., Gill, B.C., Jiang, G., Kah, L.C., Knoll, A.H., Loyd, S.J., Osburn, M.R. and Planavsky, N.J., 2017. Perspectives on Proterozoic surface ocean redox from iodine contents in ancient and recent carbonate. Earth and Planetary Science Letters, 463, pp.159-170.

Harland, W., 1964. Critical evidence for a great infra-Cambrian glaciation. Geologische Rundschau 54, 45–61.

Hawkesworth, C.J., Cawood, P.A., Dhuime, B., 2016.Tectonics and crustal evolution. GSA Today, 26(9), 4-11, doi: 10.1130/GSATG272A.1.

Hayes, J.M., 1994. Global methanotrophy at the Archean-Proterozoic transition, in: S. Bengtson (Ed.), Early life on Earth, Columbia University Press, New York, 1994, pp. 220–236.
Hazen, R.M., 2010. The evolution of minerals. Scientific American 303(3), 58-65.
Hazen, R.M., Bekker, A., Bish, D.L., Bleeker, W., Downs, R.T., Farquhar, J., Ferry, J.M., Grew, E.S., Knoll, A.H., Papoineau, D., Ralph, J.P., Sverjensky, D.A., Valley, J.W., 2011. Needs and opportunitires in mineral evolution research. American Mineralogist, 96, 953-963.
Hedberg, H., 1974. Basis for chronostratigraphic classification of the Precambrian. Precambrian Research, 1, 165-177.
Heubeck, C., Lowe, D.R., 1994. Depositional and tectonic setting of the Archean Moodies Group, Barberton greenstone belt, South Africa. Precambrian Research, 68(3-4), 257-290.
Hill, A.C., Cotter, K.L., Grey, K., 2000. Mid-Neoproterozoic biostratigraphy and isotope stratigraphy in Australia. Precambrian Research 100, 28–298.
Hill, A. C., Walter, M. R., 2000. Mid-Neoproterozoic (~830-750 Ma) isotope stratigraphy of Australia and global correlation. Precambrian Research 100, 181–211.
Hodgskiss, M.S.W., Crockford, P.W., Peng, Y., Wing, B.A., Horner, T.J., 2019. A productivity collapse to end Earth's Great Oxidation. PNAS, 116, 17207-17212, doi: 10.1073/pnas.1900325116.
Hodgkiss, M.S.W., Kunzmann, M., Poirier, A.,, Halverson, G.P., 2018. The role of microbial iron reduction in the formation of Proterozoic molar tooth structures. Earth and Planetary Science Letters, 482, 1-11.
Hofmann, H.J., 1975. Precambrian microflora, Belcher Islands, Canada: significance and systematics. Journal of Paleontology 50, 1040-1071.
Hofmann, H.J., 1990. Precambrian time units and nomenclature – the geon concept. Geology, 18, 340-341.
Hofmann, H.J., 1992. New Precambrian time scale: Comments. Epsiodes, 15(2), 122-123.
Hoffman, P. F., 1989. Speculations on Laurentia's first gigayear (2.0 to 1.0 Ga): Geology, 17, 135-138.
Hoffman, P.F., 2014. The origin of Laurentia: Rae craton as the backstop for proto-Laurentian amalgamation by slab suction: Geoscience Canada, 41, 313-320.
Hoffman, P.F., Abbott, D.S., Ashkenay, Y., Benn, D. I., Brocks, J.J., Cohen, P.A., Cox, G.M., Creveling, J.R., Donnadieu, Y., Erwin, D.H., Fairchild, I.J., Ferreira, D., Goodman, J.C., Halverson, G.P., Jansen, M.F., Le Hir, G., Love, G.D., Macdonald, F.A., Maloof, A.C., Partin, C.A., Ramstein, G., Rose, B.E.J., Rose, C.V., Sadler, P.M., Tziperman, E., Voigt, A., and Warren, S.G. (2017) Snowball Earth climate dynamics and Cryogenian geology and geobiology. Science Advances 3, e1600983.
Hoffman, P.F., Halverson, G. P., Domack, E. W., Maloof, A. C., Swanson-Hysell, N. L., Cox, G. M., 2012. Cryogenian glaciations on the southern tropical paleomargin of Laurentia (NE Svalbard and East Greenland), and a primary origin for the upper Russøya (Islay) carbon isotope excursion. Precambrian Research 206-207, 137–158.
Hoffman, P., Kaufman, A., Halverson, G., 1998. Comings and goings of global glaciations on a Neoproterozoic tropical platform in Namibia. GSA Today 8, 1–9.
Hoffman, P.F., Schrag, D.P., 2002. The snowball Earth hypothesis: testing the limits of global change. Terra Nova, 14, 129-155.
Hoffmann, K.H., Condon, D.J., Bowring, S.A., Crowley, J.L., 2004. A U-Pb zircon date from the Neoproterozoic Ghaub Formation, Namibia: Constraints on Marinoan glaciation. Geology 32, 817–820.
Holland, H.D., 1984. The Chemical Evolution of the Atmosphere and Oceans. Princeton University Press, Princeton, pp. 582.
Holland, H.D., 2006. The oxygenation of the atmosphere and oceans. Philosophical Transactions of the Royal Society B, 361: 903-915.
Horton, F., 2015. Did phosphorus derived from the weathering of large igneous provinces fertilize the Neoproterozoic ocean? Geochemistry, Geophysics, Geosystems 16, 1723–1738.
Howard, H.M., Smithies, R.H., Kirkland, C.L., Kelsey, D.E., Aitken, A., Wingate, M.T.D., Quentin de Gromard, R., Spaggiari, C.V., Maier, W.D., 2014. The burning heart: The Proterozoic geology and geological evolution of the west Musgrave region, central Australia. Gondwana Research 27, 64-94.
Huston, D.L., Mernagh, T.P., Hagemann, S.G., Doublier, M.P., Fiorentini, M.L., Champion, D.C., Jaques, A.L., Czarnota, K., Cayley, R., Skirrow, R., Bastrakov, E. (2016) Tectono-metallogenic

systems — The place of mineral systems within tectonic evolution, with an emphasis on Australian examples. Ore Geology Reviews 76, 168-210.
Idurnum et al., 1995.
James, H.L., 1972. Note 40 – Subdivision of Precambrian: an interim scheme to be used by U.S. Geological Survey. Amer. Assoc. Petrol. Geol. Bull., 56, 1128-1133.
James, H.L., 1978. Subdivision of the Precambrian - a brief review and a report on recent decisions by the Subcommissionon Precambrian Stratigraphy. Precambrian Research, 7, 193--204.
James, N.P., Narbonne, G.M., Sherman, A.G., 1998. Molar-tooth carbonates: shallow subtidal facies of the mid- to late Proterozoic. Journal of Sedimentary Research, 68, 716-722.
Javaux, E.J., Knoll, A.H., 2017. Micropaleontology of the lower Mesoproterozoic Roper Group, Australia, and implications for early eukaryotic evolution. Journal of Paleontology 91, 199–229.
Javaux, E.J., Knoll, A.H., Walter, M.R. 2001. Morphological and ecological complexity in early eukaryotic ecosystems. Nature, 412, 66-69.
Javaux, E.J., Lepot, K., 2018. The Paleoproterozoic fossil record: Implications for the evolution of the biosphere during Earth's middle-age. Earth Science Reviews, 176, 68-86.
Jing, X., Yang, Z., Evans, D.A.D., Tong, Y., Xi, Y., Wang, H., 2020. A pan-latitudinal Rodinia in the Tonian true polar wander frame. Earth and Planetary Science Letters, 530, 115880.
Johnson, T.E., Kirkland, C.L., Gardiner, N.J., Brown, M., Smithies, R.H., Santosh, M., 2019. Secular change in TTG compositions: Implications for the evolution of Archaean geodynamics. Earth and Planetary Science Letters, 505: 66-75.
Jones et al (2020)
Kah, L.C., Bartley, J.K., Teal, D. A., 2012. Chemostratigraphy of the Late Mesoproterozoic Atar Group, Taoudeni Basin, Mauritania: Muted isotopic variability, facies correlation, and global isotopic trends. Precambrian Research 200-203, 82–103.
Kamber, B.S., 2015. The evolving nature of terrestrial crust from the Hadean, through the Archean, into the Proterozoic. Precambrian Research, 258, 48-82.
Kamber, B.S., Tomlinson, E.L., 2019. Petrological, mineralogical and geochemical peculiarities of Archean cratons. Chemical Geology, 511, 123-151.
Karhu, J., Holland, H.D., 1996. Carbon isotopes and the rise of atmospheric oxygen. Geology, 24, 867-870.
Kaufman, A.J., Knoll, A.H., Narbonne, G.M., 1997. Isotopes, ice ages, and terminal Proterozoic Earth history. Proceedings of the National Academy of Sciences 95, 6600–6605.
Kendall, B., Creaser, R.A., Reinhard, C.Y., Lyons, T.W., Anbar, A.D., 2015. Transient episodes of mild environmental oxygenation and oxidative weathering during the late Archean. Science Advances, 1(10), 1500777 doi: 10.1126/sciadv.1500777.
Kennedy, M.J., Runnegar, B., Prave, A.R., Hoffmann, K.H., Arthur, M., 1998. Two or four Neoproterozoic glaciations? Geology 26, 1059–1063.
Kipp, M.A., Lepland, A., Buick, R., 2020. Redox fluctuations, trace metal enrichment and phosphogenesis in the ~2.0 Ga Zaonega Formation. Precambrian Research, 343, 105716.
Kipp, M.A., Stüeken, E.E., Bekker, A., Buick, R., 2017. Selenium isotopes record extensive marine suboxia during the Great Oxidation Event. Proceedings of the National Academy of Sciences, 114(5), pp.875-880.
Kirscher, U., Liu, Y., Li, Z. X., Mitchell, R. N., Pisarevsky, S., Denyszyn, S. W., Nordsvan, A., 2019. Paleomagnetism of the Hart Dolerite (Kimberley, Western Australia) - A two-stage assembly of the supercontinent Nuna?: Precambrian Research, 329, 170-181.
Klein, C., 2005. Some Precambrian banded iron-formations (BIFs) from around the world: Their age, geologic setting, mineralogy, metamorphism, geochemistry, and origin. American Mineralogist, 90: 1473-1499.
Knauth, P., Kennedy, M.J., 2009. The late Precambrian greening of the Earth. Nature 460, 728–732.
Knoll, A.H., Javaux, E.J., Hewitt, D., Cohen, P., 2006. Eukaryotic organisms in Proterozoic oceans. Philosophical Transactions of the Royal Society B 361, 1023–1038.
Knoll, A., Kaufman, A., Semikhatov, M., 1995. The carbon-isotopic composition of Proterozoic carbonates: Riphean successions from northwestern Siberia (Anabar Massif, Turukhansk Uplift). American Journal of Science 295, 823–850.

Knoll, A., Walter, M., Christie-Blick, N., 2004. A new period for the geological time scale. Science 305, 621–622.

Knoll, A.H., Walter, M.R., Narbonne, G.M., Christie-Blick, N., 2006. The Ediacaran Period: a new addition to the geologic time scale. Lethaia 39, 13–30.

Kulling, O., 1934. The Hecla Hoek Formation around Hinlopenstredet. Geografiska Annaler 14, 161–253.

Kump, L.R., Junium, C., Arthur, M.A., Brasier, A., Fallick, V., Lepland, A., Crne, A.E., Luo, G., 2011. Isotopic evidence for massive oxidation of organic matter following the great oxidation event. Science 334, 1694-1696.

Kunzmann, M., Schmid, S., Blaikie, T.N., Halverson, G.P., 2019. Facies analysis, sequence stratigraphy, and carbon isotope chemostratigraphy of a classic Zn-Pb host succession: The Proterozoic middle McArthur Group, McArthur Basin, Australia. Ore Geology Reviews, 106, 150-175.

Kurzweil, F., Claire, M., Thomazo, C., Peters, M., Hannington, M. and Strauss, H., 2013. Atmospheric sulfur rearrangement 2.7 billion years ago: Evidence for oxygenic photosynthesis. Earth and Planetary Science Letters, 366, 17-26.

Kuznetsov, A.B., Semikhatov, M.A., Maslov, A.V., Gorokhov, I.M., Prasolov, E.M., Krupenin, M.T., Kislova, I.V., 2006. New data on Sr- and C-isotopic chemostratigraphy of the Upper Riphean type section (southern Urals). Stratigraphy and Geological Correlation 14, 602–628.

Kuznetsov, A.B., Bekker, A., Ovchinnikova, G.V., Gorokhov, I.M., Vasilyeva, I.M., 2017. Unradiogenic strontium and moderate-amplitude carbon isotope variations in early Tonian seawater after the assembly of Rodinia and before the Bitter Springs Excursion. Precambrian Research 298, 157–173.

Kuznetsov, A.B., Semikhatov, M.A., Gorokhov, I.M., 2018. Strontium isotope stratigraphy: principles and state-of-the-art. Stratigraphy and Geological Correlation 26, 367-386.

Lee, C.T.A., Yeung, L.Y., McKenzie, N.R., Yokoyama, Y., Ozaki, K., Lenardic, A., 2016. Two-step rise of atmospheric oxygen linked to the growth of continents. Nature Geoscience, 9: 417–424

Lee, Y.Y., 1936. The Sinian glaciation in the lower Yangtze Valley. Bulletin of the Geoogical Society of China 15, 131–134.

Li, Z.X., Bogdanova, S.V., Collins, A.S., Davidson, A., DeWaele, B., Ernst, R.E., Fitsimmons, C.W., Fuck, R.A., Gladkochub, D.P., Jacons, J., Karlstrom, K.E., Lu, S., Natapov, L.M., Pease, V., Pisarevsky, S.A., Thrane, K., Vernikovsky, V., 2008. Assembly, configuration and break-up history of Rodinia: a synthesis. Precambrian Research, 160: 179-210.

Li, Z.X., Evans, D.A.D., Zhang, S., 2004. A 90° spin on Rodinia: possible causal links between the Neoproterozoic supercontinent, superplume, true polar wander and low-latitude glaciation. Earth and Planetary Science Letters 220, 409–421.

Li, Z.X., Evans, D.A.D., Halverson, G. P., 2013. Neoproterozoic glaciations in a revised global palaeogeography from the breakup of Rodinia to the assembly of Gondwanaland. Sedimentary Geology 294, 219–232.

Li, Z.X., Li, X.H., Kinny, P.D., Wang, J., 1999. The breakup of Rodinia: did it start with a mantle plume beneath South China? Earth and Planetary Science Letters 173, 171–181.

Li, Z.X., Mitchell, R.N., Spencer, C.J., Ernst, R., Pisarevsky, S., Kirscher, K., Murphy, J.B., 2019. Decoding Earth's rhythms: modulation of supercontinent cycles by longer superocean episodes. Precambrian Research, 323, 1-5 doi: 10.1016/j.precamres.2019.01.009.

Lindsay, J.F., 1987. Upper Proterozoic evaporites in the Amadeus basin, central Australia, and their role in basin tectonics. Geological Society of America Bulletin, 99, 852–865.

Lindsay, J.F., 2002. Supersequences, superbasins, supercontinents–evidence from the Neoproterozoic-Early Palaeozoic basins of central Australia. Basin Research 14, 207–223.

Lindsay, J.F., Brasier, M.D., 2002. Did global tectonics drive early biosphere evolution? Carbon isotope record from 2.6 to 1.9 Ga carbonates of Western Australian basins. Precambrian Research, 114, 1-34.

Logan, W.E., 1857. On the division of Azoic rocks of Canada into Huronian and Laurentian. Proc. Am. Assoc. Adv. Sci., 1857, 44-47.

Loron, C., Moczydłowska, M., 2017. Tonian (Neoproterozoic) eukaryotic and prokaryotic organic-walled microfossils from the upper Visingsö Group, Sweden. Palynology, 42, 220-254, doi: 10.1080/01916122.2017.1335656.

Loron, C.C., François, C., Rainbird, R.H., Turner, E.C., Borensztajn, S., Javaux, E.J., 2019b. Early fungi from the Proterozoic Era in Arctic Canada. Nature 270, 232–235.

Loron, C.C., Rainbird, R.H., Turner, E.C., Greenman, J.W., Javaux, E.J., 2019a. Organic-walled microfossils from the late Mesoproterozoic to early Neoproterozoic lower Shaler Supergroup (Arctic Canada): diversity and biostratigraphic significance. Precambrian Research 321, 349–374.

Luo, G., Ono, S., Beukes, N.J., Wang, D.T., Xie, S., Summons, R.E., 2016. Rapid oxygenation of Earth's atmosphere 2.33 billion years ago. Scientific Advances, 2: e1600134.

Lyons, T.W., Reinhard, C.T., Planavsky, N.J., 2014. The rise of oxygen in Earth's early ocean and atmosphere. Nature, 506: 307–315.

Macdonald, F.A., Halverson, G.P., Strauss, J., Smith, E., Cox, G., Sperling, E., 2012. Early Neoproterozoic basin formation in Yukon, Canada: Implications for the make-up and break-up of Rodinia. Geoscience Canada, 39, 77-100.

Macdonald, F.A., Schmitz, M.D., Crowley, J.L., Roots, C.F., Jones, D.S., Maloof, A.C., Strauss, J.V., Cohen, P.A., Johnston, D.T., Schrag, D.P., 2010. Calibrating the Cryogenian. Science 327, 1241–1243.

Macdonald, F.A., Schmitz, M.D., Strauss, J.V., Halverson, G.P., Gibson, T.M., Eyster, A., Cox, G., Mamrol, P., Crowley, J.L., 2018. Cryogenian of Yukon. Precambrian Research 319, 114–143.

Macdonald, F.A., Wordwsorth, R., 2017. Initiation of Snowball Earth with volcanic sulfur aerosol emissions. Geophysical Research Letters, 44, 1938-1946.

MacLennan, S., Park, Y., Swanson-Hysell, N., Maloof, A., Schoene, B., Gebreslassie, M., Antilla, E., Tesema, T., Alene, M., Haileab, B., 2018. The arc of the Snowball: U-Pb dates constrain the Islay anomaly and the initiation of the Sturtian glaciation. Geology 46, 539–542.

Manhes, G., Allègre, C., Dupré, C., Hamelin, B., 1980. Lead isotope study of basic-ultrabasic layered complexes: Speculations about the age of the earth and primitive mantle characteristics. Earth and Planetary Science Letters, 47, 370-382.

Martin, A.P., Condon, D.J., Prave, A.R., Lepland, A., 2013. A review of temporal constraints for the Palaeoproterozoic large, positive carbonate carbon isotope excursion (the Lomagundi-Jatuli Event. Earth Science Reviews, 127, 242-261.

Martin, A.P., Prave, A.R., Condon, D.J., Lepland, A., Fallick, A.E., Romashkin, A.E., Medvedev, P.V., Rychanchik, D.V., 2015. Multiple Palaeoproterozoic carbon burial episodes and excursions. Earth and Planetary Science Letters, 424, 226-236.

Mawson, D., 1949. The Late Precambrian ice age and glacial record of the Bibliando dome. Journal and Proceedings of the Royal Society of New South Wales 82, 150–174.

McKenzie, R.N., Hughes, N.C., Myrow, P.M, Banerjee, D.M., Deb, M., and Planavasky, N.J., 2013, New age constraints for the Proterozoic-Delhi successions of India and their implications. Precambrian Research, 238, 120–128.

McLelland, J.M., Selleck, B.W., Hamilton, M.A., Bickford, M.E., 2010. Late- to post-tectonic setting of some major Proterozoic anorthosite-mangerite-charnokite-granite (AMCG) suites. Canadian Mineralogist, 48: 729-750.

Meert, J.G., Santosh, M., 2017. The Columbia supercontinent revisited. Gondwana Research, 50, 67-83.

Melezhik, V.A., Fallick, A.E., Hanski, E.J., Kump, L.R., Lepland, A., Prave, A.R., Strauss, H., 2005. Emergence of the aerobic biosphere during the Archean-Proterozoic transition: Challenges of future research. GSA Today, 15, 11, 4-11.

Melezhik, V.A., Filippov, M.M., Romaskin, A.E., 2004. A giant Palaeoproterozoic deposit of shungite in NW Russia: Genesis and practical applications. Ore Geology Reviews, 24, 135-154.

Melezhik, V.A., Huhma, H., Condon, D.J., Fallick, A.E., Whitehouse, M.J., 2007. Temporal constraints on the Paleoproterozoic Lomagundi-Jatuli carbon isotopic event. Geology, 35, 655-658.

Merdith, A. S., Collins, A. S., Williams, S. E., Pisarevsky, S., Foden, J. D., Archibald, D. B., Blades, M. L., Alessio, B. L., Armistead, S., Plavsa, D., Clark, C., Müller, D., 2017. A full-plate global reconstruction of the Neoproterozoic. Gondwana Research 50, 84–134.

Miao, L., Moczydłowska, M., Zhu, S., Zhu, M., 2019. New record of organic-walled, morphologically distinct microfossils from the late Paleoproterozoic Changcheng Group in the Yanshan Range, North China. Precambrian Research 321, 172–198.

Mitchell, R.N., 2014. True polar wander and supercontinent cycles: implications for lithospheric elasticity an d the triaxial earth. American Journal of Science, 514, 966-979.

Mitchell, R.N., Kilian, T.M., Evans, D.A.D., 2012. Supercontinent cycles and the calculation of absolute palaeolongitude in deep time: Nature, 482, 208-211

Mitchell, R.N., Spencer, C.J., Kirscher, U., He, X.-F., Murphy, J.B., Li, Z.X., Collins, W.J., 2019. Harmonic hierarchy of mantle and lithospheric convective cycles: Time series analysis of hafnium isotopes of zircon. Gondwana Research, 75, 239-248.

Moreira, H., Seixas, L., Storey, C., Fowler, M., Lasalle, S., Stevenson, R., Lana, C., 2018. Evolution of Siderian juvenile crust to Rhyacian high Ba-Sr magmatism in the Mineiro Belt, southern São Francisco Craton. Geoscience Frontiers, 9, 977-995, doi: 10.1016/j.gsf.2018.01.009.

Nagovitsin, K., 2009. *Tappania*-bearing association of the Siberian platform: Biodiversity, stratigraphic position and geochronological constraints. Precambrian Research, 173, 137-145.

Nance, R.D., Murphy, J.B., 2018. Supercontinents and the case for Pannotia. In: Wilson, R.W., Houseman, G.A., McCaffrey, K.J.W., Doré, A.G., Buiter, S.J.H. (Eds.), Fifty Years of the Wilson Cycle Concept in Plate Tectonics 470, Geological Society, London, Special Publications, 470, 65-86.

Nance, R.D., Worsley, T.R., Moody, J.B., 1986. Post-Archean biogeochemical cycles and long-term episodicity in tectonic processes. Geology, 14, 514-518.

Nelson, L.L., Smith, E.F., Hodgin, E.B., Crowley, J.L., Schmitz, M.D., Macdonald, F.A., 2020. Geochronological constraints on Neoproterozoic rifting and onset of the Marinoan glaciation from the Kingston Peak Formation in Death Valley, California (USA). Geology, 48, doi:10.1130/G47668.1.

O'Neil, J., Carlson, R. W., Francis, D., Stevenson, R. K. (2008). Neodymium-142 Evidence for Hadean Mafic Crust. Science, 321, 1828–1832.

O'Neil, J., Carlson, R. W., Paquette, J. L., & Francis, D. (2012). Formation age and metamorphic history of the Nuvvuagittuq Greenstone Belt. Precambrian Research, 220–221, 23–44.

O'Neill, C., Lenardic, A., Condie, K.C., 2015. Earth's punctuated tectonic evolution: cause and effect. In: Roberts, N.M.W., Ven Kranendonk, M.J., Parman, S., Shirey, S., Clift, P.D. (Eds.), Continental Formation Through Time 389, Geological Society, London, Special Publications, pp. 17-40.

Ossa Ossa, F., Hofmann, A., Spangenberg, J.E., Poulton, S.W., Stueeken, E.E., Schoenberg, R., Eickmann, B., Wille, M., Butler, M., Bekker, A., 2019. Limited oxygen production in the Mesoarchean ocean. Proceedings of the National Academy of Sciences, 116, 6647-6652.

Ostrander, C.M., Nielsen, S.G., Owens, J.G., Kendall, B., Gordon, G.W., Romaniello, S.J., Anbar, A.D., 2019. Fully oxygenated water columns over continental shelves before the Great Oxidation Event. Nature Geoscience, 12, 186-191.

Ouyang, G. She, Z., Papineau, D., Wang, X., Luo, G., Li, C., 2020. Dynamic carbon and sulfur cycling in the aftermath of the Lomagundi-Jatuli Event: Evidence from the Paleoproterozoic Hutuo Supergroup, North China Craton. Precambrian Research 337, 105549.

Page et al., 2000.

Pang, K., Tang, Q., Wan, B., Yuan, X., 2020. New insights on the palaeobiology and biostratigraphy of the acritarch Trachyhystrychosphaeraaimika: a potential late Mesoproterozoic to Tonian index fossil. Palaeoworld, doi:10.1016/j.palwor.2020.02.003.

Papineau, D., 2010. Global biogeochemical change at both ends of the Proterozoic: Insights from phosphorites. Astrobiology, 10: 165-181.

Parfrey, L.W., Lahr, D.J.G., Knoll, A.H., Katz, L.A., 2011. Estimating the timing of early eukaryotic diversification with multigene molecular clocks. Proceedings of the National Academy of Sciences 108, 13624–13629.

Park, H.U., Zhai, J.H., Peng, P., Kim, J.N., Zhang, Y.B., Kim, M.C., Park, U., Feng, L.J., 2016. Deposition age of the Sangwon Supergroup in the Pyongnam basin (Korea) and the early Tonian negative carbon isotope interval. Acta Petrologica Sinica, 32, 2181-2195.

Partin, C.A., Bekker, A., Planavsky, N.J., Scott, C.T., Gill, B.C., Li, C., Podkovyrov, V., Maslov, A., Konhauser, K.O., Lalonde, S.V., Love, G.D., 2013. Large-scale fluctuations in Precambrian atmospheric and oceanic oxygen levels from the record of U in shales. Earth and Planetary Science Letters, 369, 284-293.

Partin, C.A., Bekker, A., Sylvester, P.J., Wodicka, N., Stern, R.A., Chacko, T., Heaman, L.M., 2014. Filling the juvenile magmatic gap: Evidence of uninterrupted Paleoproterozoic plate tectonics. Earth and Planetary Science Letters, 388, 123-124.

Patterson, C., 1956. Age of meteorites and the Earth. Geochimica et Cosmochimica Acta, 10, 230–237,

Peng, P., 2015. Precambrian mafic dyke swarms in the North China Craton and their geological implications. SCES, doi: 10.1007/s11430-014-5026-x.

Peng, S., Babcock, L., Ahlberg, P., 2020. The Cambrian Period. From: F.M. Gradstein, J.G. Ogg, M. Schmitz, G. Ogg). The Geologic Time Scale 2020. Elsevier Science Limited, in press.

Philippot, P., Avila, J.N., Killingsworth, B.A., Tessalina, S., Baton, F., Caquineau, T., Muller, E., Pecoits, E., Cartigny, P., Lalonde, S.V., Ireland, T.R., Thomazo, C., van Kranendonk, M.J., Busigny, V., 2018. Globally asynchronous Sulphur isotope signals require re-definition of the Great Oxidation Event. Nature Communications, 9(1), 1-10 doi: 10.1038/s41467-018-04621.

Pietrzak-Renaud, N., Davis, D., 2014. U-Pb geochronology of baddeleyite from the Belleview metadiabase: Age and geotectonic implications for the Negaunee Iron Formation, Michigan. Precambrian Research, 250, 1-5.

Pimentel, M.M., Heaman, L., Fuck, R.A., Marini, O.J. 1991. U-Pb zircon geochronology of Precambrian tin-bearing continental-type acid magmatism in central Brazil. Precambrian Research 52, 321-335, 1991.

Planavsky, N.J., Reinhard, C.T., Qang, X., Thomson, D., McGoldrick, P., Rainbird, R.H., Johnson, T., Fischer, W.W., Lyons, T.W., 2014. Low mid-Proterozoic atmospheric oxygen levels and the delayed rise of animals. Science, 346, 635-638.

Plumb, K.A., 1991. New Precambrian time scale. Episodes, 14, 139–140.

Plumb, K.A., 1992. New Precambrian time scale – reply. Episodes, 15(2), 124-125.

Plumb, K.A., James, H.L., 1986. Subdivision of Precambrian time: recommendations and suggestions by Subcommission on Precambrian stratigraphy. Precambrian Research 32, 65–92.

Porter, S.M., 2016. Tiny vampires in ancient seas: evidence for predation via perforation in fossils from the 780–740 million-year-old Chuar Group, Grand Canyon, USA. Proceedings of the Royal Society B 283, 20160221.

Poulton, S.W., Canfield, D.E., 2011. Ferruginous conditions: A dominant feature of oceans throughout Earth's history. Elements, 10.2113/gselements.7.2.107.

Porter, S.M., Knoll, A.H., 2000. Testate amoebae in the Neoproterozoic Era: evidence from vase-shaped microfossils in the Chuar Group, Grand Canyon. Paleobiology 26, 360-385.

Porter, S.M., Meisterfeld, R., Knoll, A.H., 2003. Vase-shaped microfossils from the Neoproterozoic Chuar Group, Grand Canyon: a classification guided by modern testate amoebae. Journal of Paleontology 77, 409-429.

Porter, S.M., Riedman, L.A., 2016. Systematics of organic-walled microfossils from the c. 780–740 Ma Chuar Group, Grand Canyon, Arizona. Journal of Paleontology 90, 815–853.

Poulton, S.W., Fralick, P.W., Canfield, D.E., 2004. The transition to a sulphidic ocean approximately 1.84 billion years ago, Nature, 431,173-177.

Pourteau, A., Smit, M.A., Li, Z.X., Collins, W.J., Nordsvan, A.R., Volante, S., Li, J., 2018. 1.6 Ga crustal thickening along the final Nuna suture: Geology, 46, 959-962.

Prave, A.R., Condon, D.J., Hoffmann, K.H., Tapster, S., Fallick, A.E., 2016. Duration and nature of the end-Cryogenian (Marinoan) glaciation. Geology 44, 631–634.

Prince, J.K.G., Rainbird, R. H., Wing, B.A., 2019. Evaporite deposition in the mid-Neoproterozoic as a driver for changes in seawater chemistry and the biogeochemical cycle of sulfur. Geology, 47(4), 291-294. doi: 10.1130/G45464.1,

Puetz, S.J., Condie, K., 2019. Time series analysis of mantle cycles Part 1: Periodicities and correlations among seven global isotopic databases. Geoscience Frontiers, 10, 1305-1326.

Qu et al., 2014.

Rainbird, R.H., Jefferson, C.W., Young, G.M., 1996. The early Neoproterozoic sedimentary succession B of northwestern Laurentia: Correlations and paleogeographic significance. Geological Society of America Bulletin 108, 454–470.

Ranjan, S., Upadhyay, D., Pruseth, K.L., Nanda, J.K., 2020. Detrital zircon evidence for change in geodynamic regime of continental crust formation 3.7-3.6 billion years ago. Earth and Planetary Science Letters, 538, 116206 doi: 10.1016/j.epsl.2020.116206.

Rawlings, D.J., 1999. Stratigraphic resolution of a multiphase intracratonic basin system: the McArthur Basin, northern Australia. Australian Journal of Earth Sciences, 46(5), 703-723. doi: 10.1046/j.1440-0952.1999.00739.x.

Ray, J.S., 2006. Age of the Vindhyan Supergroup: A review of recent findings. Journal of Earth System Science 115, 149–160.

Reusch, H., 1891. SkuringmaerkerogmoraenguseftervistiFinnmarkenfraenperiodemegetaeldre end 'istiden' (Glacial striae and boulder-clay in Norwegian Lapponie from a period much older than the last ice age). Norges Geologiske Undersøkelse 1, 78–85, 97–100.

Riding, R., 2008. Abiogenic, microbial and hybrid authigenic carbonate crusts: components of Precambrian stromatolites. Geologia Croatia, 61, 73-103.

Riding, R., Fralick, P., Liang, L., 2014. Identification of an Archean marine oxygen oasis. Precambrian Research 251, 232-237.

Riedman, L.A., Porter, S., 2016. Organic-walled microfossils of the mid-Neoproterozoic Alinya Formation, Officer Basin, Australia. Journal of Paleontology 90, 854-887.

Riedman, L.A., Porter, S.M., Calver, C.R., 2018. Vase-shaped microfossil biostratigraphy with new data from Tasmania, Svalbard, Greenland, Sweden and the Yukon. Precambrian Research 319, 19-36.

Riedman, L.A., Sadler, P.M., 2018. Global species richness record and biostratigraphic potential of early to middle Neoproterozoic eukaryote fossils. Precambrian Research 319, 6-18.

Rivers, T., 2015. Tectonic Setting and Evolution of the Grenville Orogen: An Assessment of Progress Over the Last 40 Years. *Geoscience Canada*, *42*(1), 77-124, doi:10.12789/geocanj.2014.41.057

Rogers, J.J.W., Santosh, M., 2002. Configuration of Columbia: a Mesoproterozoic supercontinent. Gondwana Research, 5: 5-22.

Rooney, A.D., Strauss, J.V., Brandon, A.D., Macdonald, F.A., 2015. A Cryogenian chronology: Two long-lasting synchronous Neoproterozoic glaciations. Geology 43, 459–462.

Rooney, A.D., Yang, C., Condon, D.J., Zhu, M., Macdonald, F.A., 2020. U-Pb and Re-Os geochronology tracks stratigraphic condensation in the Sturtian snowball Earth aftermath. Geology, 48(6), 625-629. doi: 10.1130/G47246.1

Safanova, L., Maruyama, S., 2014. Asia: a frontier for a future supercontinent Amasia. International Geology Reviews, 56: 1051-1071.

Sánchez-Baracaldo, P., Raven, J.A., Pisani, D., Knoll, A.H., 2017. Early photosynthetic eukaryotes inhabited low-salinity habitats. Proceedings of the National Academy of Sciences, 114(37), pp.E7737-E7745.

Satkoski, A.M., Lowe, D.R., Beard, B.L., Coleman, M.L., Johnson, C.M., 2016. A high continental weathering flux into Paleoarchean seawater revealed by strontium isotope analysis of 3.26 Ga barite. Earth and Planetary Science Letters, 454: 28–35.

Scott, C., Lyons, T.W., Bekker, A., Shen, Y.A., Poulton, S.W., Chu, X.L., Anbar, A.D., 2008. Tracing the stepwise oxygenation of the Proterozoic ocean. Nature, 452, 456-459.

Schroeder, S., Bekker, A., Beukes, N.J., Strauss, H., van Niekerk, H.S., 2008. Rise in seawater sulphate concentrations associated with the Paleoproterozoic positive carbon isotope excursion: evidence from sulphate evaporites in the ~2.2-2.1 Gyr shallow-marine Lucknow Formation, South Africa. Terra Nova, 20, 108-117.

Schulze, D.J., Harte, B., Edinburgh Ion Microprobe Facility Staff, Page, Z., Valley, J.W., Channer, D.M., Jaques, A.L., 2013. Anticorrelation between low $\delta^{13}C$ of eclogitic diamonds and high $\delta^{18}C$ of their coesite and garnet inclusions requires a subduction origin. Geology 41, 455-458.

Sedgwick, A., 1845. On the Older Palæozoic (Protozoic) Rocks of North Wales. Quarterly Journal of the Geological Society, 1, 5-22.

Semikhatov, M.A., Kuznetsov, A.B., Chumakov, N.M., 2015. Isotope age boundaries between the general stratigraphic subdivisions of the upper Proterozoic (Riphean and Vendian) in Russia: The evolution of opinions and the current estimate. Stratigraphy and Geological Correlation, 23, 568-579.

Sergeev, V.N., Vorob'eva, N.G., Petrov, P.Y., 2017. The biostratigraphic conundrum of Siberia: do true Tonian–Cryogenian microfossils occur in Mesoproterozoic rocks? Precambrian Research 299, 282–302.

Shang, M., Tang, D., Shi, X., Zhou, L., Zhou, X., Song, H., Jiang, G., 2019. A pulse of oxygen increase in the early Mesoproterozoic ocean at ca. 1.57-1.56 Ga. Earth and Planetary Science Letters, 527, 115797.

Sharma, Mukund, Shukla, Y. 2009. Taxonomy and affinity of Early Mesoproterozoic megascopically helically coiled and related fossils from the Rohtas Formation, the Vindhyan Supergroup, India. Precambrian Research, 173, 105–122.

Shen, Y., Canfield, D. E. and Knoll, A. H. 2002. Middle Proterozoic ocean chemistry: evidence from the McArthur Basin, northern Australia. American Journal of Science, 302, 81-109.

Shields, G.A., 2002. 'Molar-tooth microspar': a chemical explanation for its disappearance ~750 Ma. Terra Nova, 14, 108-113.

Shields, G.A., 2007. A normalised seawater strontium isotope curve: possible implications for Neoproterozoic-Cambrian weathering rates and the further oxygenation of the Earth. eEarth, 2: 35-42.

Shields, G.A., Halverson, G.P., Porter, S.M., 2018. Descent into the Cryogenian. Precambrian Research 319, 1–5.

Shields, G.A., Mills, B.J.W., 2017. Tectonic controls on the long-term carbon isotope mass balance. PNAS, doi:10.1073/pnas.1614506114.

Shields, G.A., Mills, B.J.W., Zhu, M., Daines, S., Lenton, T.M., 2019. Unique Neoproterozoic carbon isotope excursions sustained by coupled evaporite dissolution and pyrite burial. Nature Geoscience, 12, 823-827. doi: 10.1038/s41561-019-0434-3.

Shields, G., Veizer, J., 2002, Precambrian marine carbonate isotope database: Version 1.1: Geochemistry Geophysics Geosystems, 3(6), 1–12, doi: 10.1029/2001GC000266.

Shields-Zhou, G.A., Hill, A.C., Macbabhann, B.A., 2012. The Cryogenian Period. Chapter 17 in F.M. Gradstein, J. G. Ogg, M. Schmitz, and G. Ogg (Eds.), The Geological Time Scale 2012 (vol. 1). Elsevier, pp. 393–411.

Shields-Zhou, G., Porter, S.A., Halverson, G.P., 2016. A new rock-based definition for the Cryogenian Period (circa 720–635 Ma). Episodes 39, 3–9.

Shirey, S.B., Richardson, S.H., 2011. Start of the Wilson Cycles at 3 Ga shown by Diamonds from Subcontinental Mantle. Science, 333, 434-458.

Singh, V. K., Sharma Mukund, Sergeev V. N. 2019. A New Record of Acanthomorphic Acritarch *Tappania* Yin from the Early Mesoproterozoic Saraipali Formation, Singhora Group, Chhattisgarh Supergroup, India and its Biostratigraphic Significance. Journal of the Geological Society of India, 94, 471-479.

Slack, J.F., Grenne, T., Bekker, A., Rouxel, O.J., Lindberg, P.A., 2007. Suboxic deep seawater in the late Paleoproterozoic: evidence from hematitic chert and Fe formation related to seafloor hydrothermal sulfide deposits, central Arizona, USA. Earth and Planetary Science Letters, 255, 243-256.

Spencer, C.J., Hawkesworth, C., Cawood, P.A., Dhuime, B., 2013. Not all supercontinents are created equal: Gondwana-Rodinia case study. Geology, 41(7), 795–798.

Spencer, C.J., Murphy, J.B., Kirkland, C.L., Liu, Y., Mitchell, R.M., 2018. A Palaeoproterozoic tecton-magmatic lull as a potential trigger for the supercontinent cycle. Nature Geoscience, 11: 97-101.

Spencer, C.J., 2020. Continuous continental growth as constrained by the sedimentary record. American Journal of Science, 320, 373-401.

Sprigg, R.C., 1947. Early Cambrian (?) jellyfishes from the Flinders Ranges, South Australia. Transactions of the Royal Society of South Australia, 71, 212–224.

Stockwell, C.H., 1961. Structural provinces, orogenies, and time classification of rocks of the Canadian Precambrian Shield. Geol. Surv. Canada. Paper, 61-17, 108-118.

Stockwell, C.H., 1982. Proposals for time classification and correlation of Precambrian rocks and events in Canada and adjacent areas of the Canadian Shield. Part 1: A time classification of Precambrian rocks and events. Geol. Surv. Can. Pap. 80-19.

Stolper, D.A.., Brenhin-Keller, C., 2018. A record of deep-ocean dissolved O_2 from the oxidation state of iron in submarine basalts. Nature, doi:10.1038/nature/25009.

Strachan, R., Murphy, J.B., Darling, J., Storey, C., Shields, G.A., 2020. Precambrian (4.56–1.0 Ga). From: F.M. Gradstein, J.G. Ogg, M. Schmitz, G. Ogg). The Geologic Time Scale 2020. Elsevier Science Limited, in press.

Strauss, J.V., Rooney, A.D., Macdonald, F.A., Brandon, A.D., Knoll, A.H., 2014. 740 Ma vase-shaped microfossils from Yukon, Canada: implications for Neoproterozoic chronology and biostratigraphy: Geology, 42, 659–662.

Swanson-Hysell, N. L., Maloof, A. C., Condon, D. J., Jenkin, G. R. T., Alene, M., Tremblay, M. M., Tesema, T., Rooney, A. D., Haileab, B., 2015. Stratigraphy and geochronology of the Tambien Group, Ethiopia: Evidence for globally synchronous carbon isotope change in the Neoproterozoic. Geology 43, 323–326.

Swanson-Hysell, N. L., Maloof, A. C., Kirschvink, J. L., Evans, D. A. D., Halverson, G. P., Hurtgen, M. T., 2012. Constraints on Neoproterozoic paleogeography and Paleozoic orogenesis from paleomagnetic records of the Bitter Springs Formation, central Australia. American Journal of Science 312, 817–884.

Tang, H., Chen, Y., 2013. Global glaciations and atmospheric change at c. 2.3 Ga. Geoscience Frontiers, 4: 583-596.

Tang, Q., Pang, K., Xiao, S., Yuan, X., Ou, Z., Wan, B., 2013. Organic-walled microfossils from the early Neoproterozoic Liulaobei Formation in the Huainan region of North China and their biostratigraphic significance. Precambrian Research 236, 157–181.

Tang, Q., Pang, K., Yuan, X., Wan, B., Xiao, S., 2015. Organic-walled microfossils from the TonianGouhou Formation, Huaibei region, North China Craton, and their biostratigraphic implications. Precambrian Research 266, 296–318.

Tang, D., Shi, X., Wang, X., Jiang, G., 2016. Extremely low oxygen concentration in mid-Proterozoic shallow seawaters. Precambrian Research, 276, 145-157.

Tang, Q., Pang, K., Yuan, X., Xiao, S., 2020. A one-billion-year-old multicellular chlorophyte. Nature Ecology and Evolution, doi: 10.1038/s41559-020-1122-9.

Teixeira, W., Geraldes, M.C., Matos, R., Salina Ruiz, A., Saes, G., Vargas-Mattos, G., 2010. A review of the tectonic evolution of the Sunsas Belt, SW Amazonian craton. Journal of South American Earth Sciences, 29, 47-60.

Thomazo, C., Pinto, D.L., Busigny, V., Ader, M., Hashizume, K., Philippot, P., 2009. Biological activity and the Earth's surface evolution: insights from carbon, sulfur, nitrogen and iron stable isotopes in the rock record. Comptes Rendus Palevol, 8, 665-678.

Thomson, J., 1871. On the stratified rocks of Islay. Report of the 41st Meeting of the British Association for the Advancement of Science, Edinburgh, John Murray, London, pp. 110-111.

Thomson, J., 1877. On the geology of the island of Islay. Transactions of the Geological Society of Glasgow 5, 200-222.

Thomson, D., Rainbird, R.H., Planavsky, N., Lyons, T.W., Bekker, A., 2015. Chemostratigraphy of the Shaler Supergroup, Victoria Island, NW Canada: a record of ocean composition prior to the Cryogenian glaciations. Precambrian Research, 263, 232-245.

Torres, M.A., Paris, G., Adkins, J.F., Fischer, W.W., 2018. Riverine evidence for isotopic mass balance in the Earth's early sulfur cycle. Nature Geoscience, 11, 661-664.

Trendall, A.F., 1966. Towards rationalism in Precambrian stratigraphy. Geol. Soc. Austr. J., 13, 517-522.

Trendall, A.F., 1991. The "Geological Unit" (g.u.) – A suggested new measure of geologic time. Geology, 19, 195.

Trendall et al. (2004)

Tsikos, H., Matthews, A., Erel, Y., Moore, J.M., 2010. Iron isotopes constrain biogeochemical redox cycling of iron and manganese in a Palaeoproterozoic stratified basin. Earth and Planetary Science Letters, 298, 125-134.

Tyrell, T. 1999. The relative influences of nitrogen and phosphorus on oceanic primary production. Nature 400, 525–531.

Van Kranendonk, M.J., Altermann, W., Beard, B.L., Hoffman, P.E., Johnson, C.J., Kasting, J.F., Melezhik, V.A., Nutman, A.P., Papineau, D., Pirajino, F., 2012. A chronostratigraphic division of the Precambrian: possibilities and challenges. In: Gradstein, F.M., Ogg, J.G., Schmitz, M., Ogg, G., (Coordinators). The Geologic Time Scale 2012. Elsevier Publ., pp. 299-392.

Van Kranendonk, M.J., Kirkland, C.L., 2016. Conditioned duality of the Earth system: Geochemical tracing of the supercontinent cycle through Earth history. Earth-Science Reviews, 160: 171-187.

Veizer, J., 1989. Strontium isotopes in seawater through time. Annual Reviews of Earth and Planetary Sciences, 17, 141-167.

Vermeesch, P., Resentini, A., and Garzanti, E., 2016. An R package for statistical provenance analysis: Sedimentary Geology, 336, 14–25, https://doi.org/10.1016/j.sedgeo.2016.01.009

Walker, J.C.G., Hays, P.B., and Kasting, J.F., 1981. A negative feedback mechanism for the long-term stabilization of Earth's surface temperature: Journal of Geophysical Research, 86, 9776, doi:10.1029/JC086iC10p09776.

Walter, M. R., Oehler, J. H., and Oehler, D. Z. 1976. Megascopic algae 1300 million years old from the Belt Supergroup, Montana: a reinterpretation of Walcott's Helminthoidichnites. Journal of Paleontology 50, 872–881.

Wang, X. C., Li, Z. X., Li, X. H., Li, Q. L., Zhang, Q.-R., 2011. Geochemical and Hf-Nd isotope data of Nanhua rift sedimentary and volcaniclastic rocks indicate a Neoproterozoic continental flood basalt provenance. Lithos, 427–440.

Wang, C., Peng, P., Wang, X., Yang, S., 2016. Nature of three Proterozoic (1680 Ma, 1230 Ma and 775 Ma) mafic dyke swarms in North China: Implications for tectonic evolution and paleogeographic reconstruction. Precambrian Research, 285, 109-126.

Wang, D., Zhu, X.-K., Zhao, N., Yan, B., Li, X.-H., Shi, F., Zhang, F., 2019. Timing of the termination of Sturtian glaciation: SIMS U-Pb zircon dating from South China. Journal of Asian Earth Sciences 177, 287–294.

Ward, L.M., Kirschvink, J.L., Fischer, W.W., 2016. Timescales of oxygenation following the evolution of oxygenic photosynthesis. Origin of Life and Evolution of the Biosphere, 46, 51-65.

Warke, M.R., Strauss, H., Schröder, S., 2020a. Positive cerium anomalies imply pre-GOE redox stratification and manganese oxidation in Paleoproterozoic shallow marine environments. Precambrian Research, 344, 105767.

Warke, M.R., Di Rocco, T., Zerkle, A.L., Lepland, A., Prave, A.R., Martin, A.P., Ueno, Y., Condon, D.J., Claire, M.W., 2020b. The Great Oxidation Event preceded a Paleoproterozoic Snowball Earth. Proceedings of the National Academy of Sciences, 117, 13314-13320.

Whitmeyer, S.J., Karlstrom, K.E., 2007. Tectonic model for the Proterozoic growth of North Americ. Geosphere, 3: 220-259.

Worsley, T.R., Nance, R.D., Moody, J.B., 1985. Proterozoic to recent tectonic tuning of biogeochemical cycles. In: Sunquist, E.T., Broecker, W.S. (Eds.), The Carbon Cycle and Atmospheric CO_2: Natural Variations Archean to Present. American Geophysical Union, Geophysical Monographs, 32: 561-572.

Xiao, S., Narbonne, G.M., 2020. The Ediacaran Period. From: F.M. Gradstein, J.G. Ogg, M. Schmitz, G. Ogg). The Geologic Time Scale 2020. Elsevier Science Limited, in press.

Xiao, S., Tang, Q., 2018. After the boring billion and before the freezing millions: evolutionary patterns and innovations in the Tonian Period: Emerging Topics in Life Sciences, 2, 161-171, doi: 10.1042/ETLS20170165.

Yin, L. 1997. Acanthomorphic acritarchs from Meso-Neoproterozoic shales of the Ruyang Group, Shanxi, China. Rev. Palaeobot. Palynol., 98: 15-25.

Yin, L., Changtai, N., Kong, F.-F. 2018. A Review of Proterozoic Organic walled Microfossils – *Tappania* and Its Biologic and Geologic Implication. Acta Palaeontol. Sinica, 57: 147-156.

Young, G.M., 2013. Precambrian supercontinents, glaciations, atmospheric oxygenation, metazoan evolution and an impact that may have changed the second half of Earth history. Geoscience Frontiers, 4: 247-261.

Young, G.M., 2019. Aspects of the Archean-Proterozoic transition: How the great Huronian Glacial Event was initiated by rift-related uplift and terminated at the rift-drift transition during break-up of Lauroscandia. Earth Science Reviews, 190, 171-189.

Zalasiewicz, J. Smith, A., Brenchley, P., Evans, J., Knox, R., Riley, N., Gale, A., Gregory, F.J., Rushton, A., Gibbard, P., Hesselbo, S., Marshall, J., Oates, M., Rawson, P., Trewin, N., 2004. Simplifying the stratigraphy of time. Geology, 32, 1-4.

Zhai, M.G., Hu, B., Zhao, T.P., Peng, P., Meng, Q.R., 2015. Late Paleoproterozoic-Neoproterozoic multi-rifiting events in the North China craton and their geological significance: a study advance and review. Tectonophysics, 662, 153-166.

Zhang, K., Zhu, X., Wood, R.., Shi, Y., Gao, Z., Poulton, S.W., 2018. Oxygenation of the Mesoproterozoic ocean and the evolution of complex eukaryotes. Nature Geoscience, 11: 345-350.

Zhang, S., Wang, X., Wang, H., Bjerrum, C.J., Hammerlund, E.U., Mafalda Costa, M., Connelly, J.N., Zhang, B., Su, J., Canfield, D.E., 2016. Sufficient oxygen for animal respiration 1,400 million years ago. Proceedings of the National Academy of Science, 113, 1731-1736.

Zhang, S., Ernst, R.E., Pei, J., Zhao, Y., Zhou, M., Hu, G., 2018. A temporal and causal link between c. 1380 Ma large igneous provinces and black shale: Implications for the Mesoproterozoic time scale and paleoenvironment. Geology, 46: 963-966.

Zhao, G., Cawood, P.A., 2012. Precambrian geology of China. Precambrian Research, 222-223, 13-54.

Zhao, G., Cawood, P.A., Wilde, S.A., Sun, M., 2002. Review of global 2.1-1.8 Ga orogens: implications for a pre-Rodinia supercontinent. Earth-Science Reviews, 59, 125-162.

Zhou, C.M., Huyskens, M.H., Lang, X.G., Xiao, S.H., Yin, Q.Z., 2019. Calibrating the terminations of Cryogenian global glaciations: Geology, 47, 251–254, doi: 10.1130/G45719.1.

Zhou, Y., Pogge von Strandmann, P.A.E., Zhu, M., Ling, H., Manning, C., Li, D., He, T., Shields, G.A., 2020. Reconstructing Tonian seawater $^{87}Sr/^{86}Sr$ using calcite microspar. Geology, doi: 10.1130/G46756.1.

Zhu, S., Zhu, M., Knoll, A.H., Yin, Z., Zhao, F., Sun, S., Qu, Y., Shi, M., Liu, H., 2016. Decimetre-scale multicellular eukaryotes from the 1.56-billion-year-old Gaoyuzhuang Formation in North China. Nature Communications, doi: 10.1038/ncomms11500.

Zumberge, J.A., Rocher, D., Love, G.D., 2019. Free and kerogen-bound biomarkers from late Tonian sedimentary rocks record abundant eukaryotes in mid-Neoproterozoic marine communities. Geobiology, doi: 10.1111/gbi.12378.